

See discussions, stats, and author profiles for this publication at: <https://www.researchgate.net/publication/273123335>

Recent research progress on tropical cyclone structure and intensity

Article · May 2012

DOI: 10.6057/2012TCRR02.05

CITATIONS
44

READS
6,287

1 author:



Yuming Wang
University of Hawai'i at Mānoa
264 PUBLICATIONS 10,847 CITATIONS

[SEE PROFILE](#)

Some of the authors of this publication are also working on these related projects:

- Project Tropical Cyclone Intensification [View project](#)
- Project Regional Climate [View project](#)

RECENT RESEARCH PROGRESS ON TROPICAL CYCLONE STRUCTURE AND INTENSITY

YUQING WANG

*International Pacific Research Center and Department of Meteorology, School of Ocean and Earth
Science and Technology, University of Hawaii at Manoa, Honolulu, HI 96822, USA*

ABSTRACT

This article provides a balanced, brief review on the research progress in the area of tropical cyclone (TC) structure and intensity achieved in the past three decade. Efforts have been made to introduce basic concepts and new findings relevant to the understanding of TC structure and intensity in ways as simple and appreciate as possible. After a brief discussion on the axisymmetric and asymmetric structure of mature TCs, progress in our understanding of spiral rainbands, concentric eyewall cycle, annular hurricane structure, and the inner-core size of TCs is highlighted. This is followed by discussions on the maximum potential intensity (MPI) of TCs and factors that limit TC maximum intensity. Some important remaining issues that need to be studied and addressed in the near future by the research community are identified and briefly discussed as well.

Keywords: Tropical Cyclone, Structure, Intensity

1. Introduction

Tropical cyclones (TCs) are warm-cored, intense cyclonic, atmospheric vortices that develop over the warm tropical oceans and have a horizontal scale typical of hundreds to 1000 km and extend throughout the depth of the troposphere. An intense mature TC generally consists of an eye with weak subsidence near its center surrounded by rapid swirling flow where deep convective ring slopes radially outward with height. Although an intense TC is highly axisymmetric, considerable asymmetric structures are often observed even in the inner-core region where the inertial stability is extremely high. Another distinct feature of an intense TC is the existence of active spiral rainbands outside the convective eyewall. Depending on their fundamental differences in dynamics and thermodynamics, these rainbands can be classified into inner rainbands and outer rainbands. The activity of these rainbands could induce significant structure and intensity changes of a TC.

An important concept in the literature is the existence of a theoretical upper bound in the intensity that a TC can potentially achieve given favorable environmental thermodynamic structure of the underlying ocean and the atmosphere. This intensity is commonly called the maximum potential intensity (MPI). There have been

several MPI theories proposed in the literature. However, because of various assumptions used in deriving them or because some parameters in the theories are not observationally constrained, currently available MPI theories have some limitations and seem to underestimate the actual MPI. On the other hand, because of the existence of various unfavorable environmental conditions and the internal dynamics, even though there exists an MPI for any given TC, only a very small portion of TCs in observations can reach their corresponding MPIs. Therefore, it is also an important research area to understand what limits the TC intensity in nature.

In this review article, the author will provide a recent literature review on the research progress in the area of the structure and intensity of mature TCs. The structure will be discussed in section 2, including axisymmetric and asymmetric structures, spiral rainbands, the concentric eyewall cycle, annular hurricane structure, and TC inner-core size. Section 3 will focus on TC intensity, including our current understanding of the MPI theories and factors that limit TC intensity. Some related issues that need immediate attentions by the research community for future studies will be briefly discussed in section 4. Concluding remarks will be given in the last section.

2. Tropical Cyclone Structure

In this section, recent research progress on TC structure will be reviewed. After a brief discussion on the axisym-

Corresponding author address: Dr. Yuqing Wang, IPRC/SOEST, POST 409G, 1680 East-West Road, Honolulu, HI 96822, USA. Email: yuqing@hawaii.edu

metric and asymmetric structure of mature TCs, some extended discussions will be given to spiral rainbands, concentric eyewalls, annular hurricane structures, and TC inner-core size.

a. Axisymmetric Structure

To the first order, the primary circulation of an intense TC can be considered as a warm-cored, quasi-axisymmetric vortex in gradient wind and hydrostatic balance except in the frictional boundary layer near the surface and the outflow layer in the upper troposphere. Superimposed on the primary circulation is a secondary (transverse) circulation (radial and vertical circulation) which is a result of the response to both diabatic heating and momentum forcing including surface friction. The secondary circulation transports high absolute angular momentum inward to spin up or maintain the TC primary circulation against the angular momentum loss to the ocean surface below. The warm core structure in the mid-upper troposphere and the gradient or thermal wind balance imply a decrease of tangential wind with height above the boundary layer. This broad view of a TC however does not provide any information on what determines the radial location where the maximum wind occurs, namely the radius of maximum wind (RMW), what determines the outward slope of the eyewall, and what determines the vertical decaying rate of the maximum tangential wind.

A previous observational study by Shea and Gray (1973) claimed that the outward slope of the RMW (thus the eyewall) decreases with increasing the storm intensity and decreasing the RMW itself (or thus the size of the eyewall) based on flight-level data. This earlier result was revisited by Stern and Nolan (2009) based on both observations and theoretical consideration. They showed that the outward

slope of the RMW increases with increasing the RMW itself (Fig. 1) while is not correlated with the TC intensity. The outward slope of the RMW is shown to closely follow the absolute angular momentum (AAM) surface above the boundary layer, consistent with the steady-state TC model of Emanuel (1986). Note that although no relationship is found between the vertical slope of the RMW and intensity, since the intensification of a TC is generally accompanied by the eyewall contraction, the outward slope of the eyewall may decrease as the storm intensifies.

Stern and Nolan (2011) also examined the vertical decay rate of the maximum tangential winds in TCs. They found that the vertical profile of the normalized maximum tangential wind above the inflow boundary layer shares a common shape that is nearly independent of both the storm intensity and the RMW. They also found that considerable deviations exist partly due to the supergradient/subgradient motions associated with the unbalanced flow in the inflow boundary layer forced by surface friction as discussed in Kepert (2001) and Kepert and Wang (2001). The findings of Stern and Nolan (2009 and 2011) could have some practical implications for the initialization of 3-dimensional TC structure in high-resolution dynamical models since currently we have no sufficient observations to determine the initial vertical structure and outward slope of TC eyewalls.

b. Waves and Asymmetric Structure in the Eyewall

Although the inner core structure of an intense TC is quasi-axisymmetric, considerable asymmetric structures are often observed (Fig. 2). They are characterized by propagating vortex Rossby waves (VRWs), mesovortices and polygonal eyewalls resulting from dynamical instability, or externally forced convective asymmetries (see Wang and Wu 2004 for an earlier review; Corbosiero and Molinari 2002, 2003). These asymmetries in the inner core may limit TC intensity (Wang 2002a,b; Wu and Braun 2004; and Yang et al. 2007).

The asymmetries in the inner-core are predominantly associated with the activities of VRWs whose restoring force is the radial potential vorticity (PV) gradient of the axisymmetric TC vortex (Montgomery and Kallenbach 1997). The characteristics of the VRWs and their coupling with eyewall convection and the activity of inner spiral rainbands have been extensively studied (Wang 2001, 2002a,b; Chen and Yau 2001). There are two types of VRWs, namely the sheared VRWs and the discrete VRWs or modes (Nolan and Montgomery 2002). While the sheared VRWs are responsible for the activity of inner spiral rainbands, discrete VRWs in the eyewall of a TC are responsible for the formation of the polygonal eyewall structure and eyewall mesovortices (Schubert et al. 1999; Reasor et al. 2000; Kossin and Schubert 2001; Montgomery et al. 2002; Kossin et al. 2002; Kossin and Schubert 2004; Kwon and Frank 2005; Rozoff et al. 2009; Hendricks et al. 2009; Hendricks and Schubert 2010).

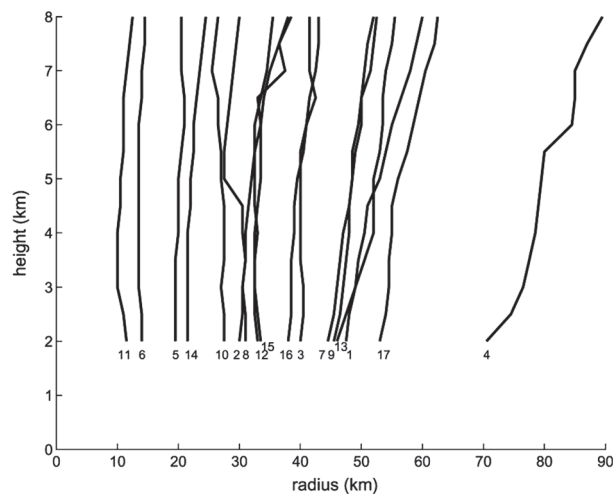


FIG. 1. Radius of maximum wind (RMW) versus height for 17 hurricane cases over the North Atlantic (from Stern and Nolan 2009). (Numbers are for different cases shown in their Table 1).

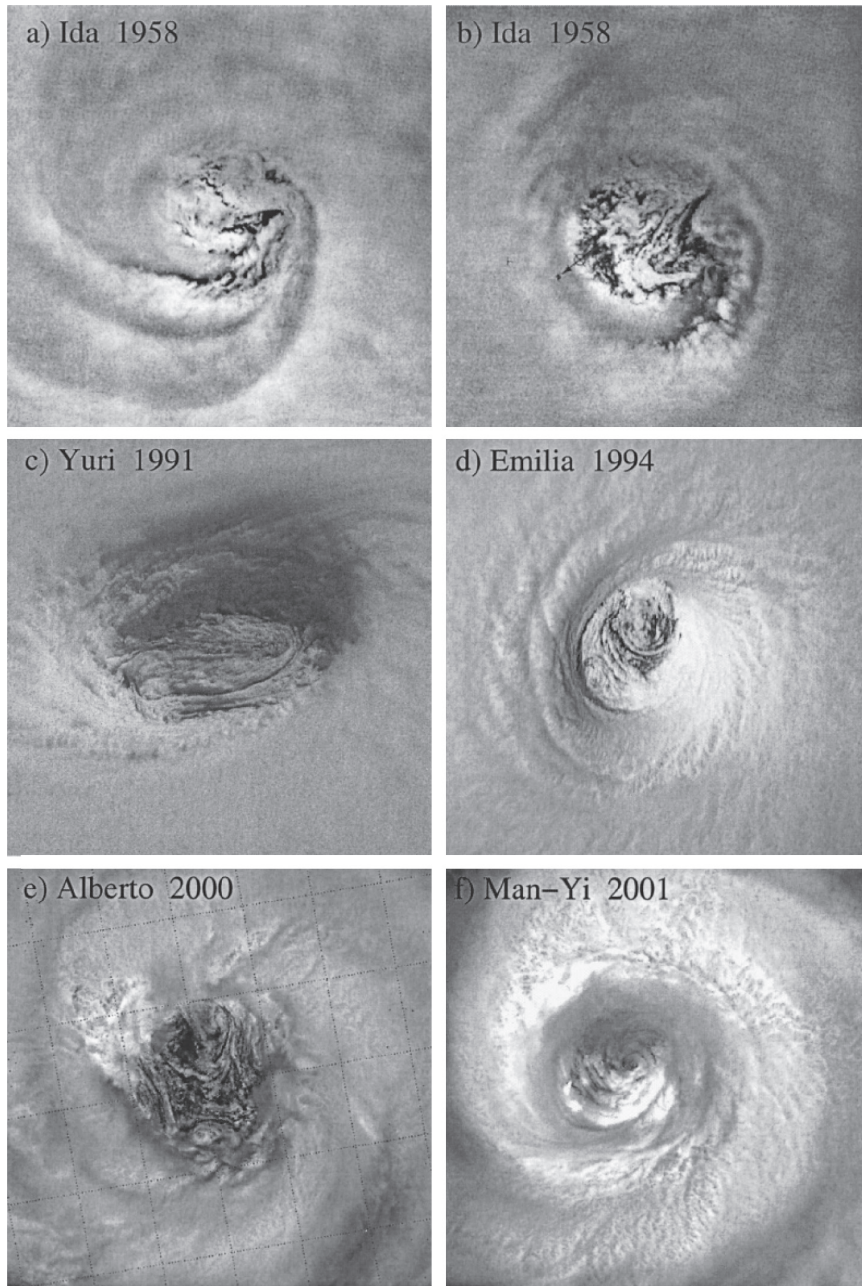


FIG. 2. Montage of images showing a variety of swirling patterns in hurricane eye clouds: (a), (b) high-altitude U-2 aircraft photographic reconnaissance, (c), (d) taken from the space shuttle, (e), (f) MODIS images (from Kossin et al. 2002).

In idealized full-physics model simulations, Wang (2001, 2002a,b) and Chen and Yau (2001) showed that cyclonic PV anomalies (VRWs) propagate azimuthally with a phase speed much slower than the local tangential wind speed and are coupled with elevated radar reflectivity in the inner rainbands, indicative of a strong connection between VRWs and inner rainbands. Observational studies also support the VRW dynamics view of inner spiral rainbands (Reasor et al. 2000; Corbosiero et al. 2006). By examining the asym-

metric structure of Hurricane Elena (1985), Corbosiero et al. (2006) showed that repeated inner bands were emanated from the eyewall and propagated azimuthally with an average azimuthal phase speed of ~68% of the local tangential wind speed and radially outward with the existence of a stagnation radius, qualitatively consistent with the theoretical prediction of VRWs by Montgomery and Kallenbach (1997).

Montgomery and Kallenbach (1997) formulated a local

dispersion relation for VRWs in a two-dimensional non-divergent barotropic model and an asymmetric balanced shallow-water model. Möller and Montgomery (2000) further extended those results to a three-dimensional stably stratified barotropic circular vortex in gradient wind balance. The derived local dispersion relation is

$$\omega = n\bar{\Omega} + \frac{n}{R} \frac{\bar{\xi}}{\bar{q}} \frac{\bar{q}'(R)}{[k^2 + \frac{n^2}{R^2} + (\bar{\eta}\bar{\xi}m^2)/N^2]}, \quad (1)$$

where ω is the local wave frequency, variables with an overbar indicate the mean state quantities of the circular barotropic vortex, n is the azimuthal wavenumber, m the vertical wavenumber, k the time-dependent radial wavenumber [$k = k_0 - nt\bar{\Omega}'(R)$], $\bar{\Omega}$ is the mean angular velocity, $\bar{\Omega}'(R)$ is the radial gradient of the mean angular velocity, R is the reference radius, $\bar{\eta}$ is the mean absolute vorticity, $\bar{\xi}$ is the mean inertial parameter, N^2 is the static stability, and \bar{q} and $\bar{q}'(R)$ denote the mean PV and its radial gradient at radius R .

From (1), we can see that VRWs in the form of a trailing spiral travel azimuthally in a retrograde sense relative to the local tangential winds for a negative effective beta (radial PV gradient). The retrograde phase speed is smaller for baroclinic VRW than for barotropic VRWs since the inertial stability ($\bar{\eta}\bar{\xi}$) is generally positive and large in the TC core. Li and Wang (2012a,b) showed that the actual phase speed of VRWs is generally faster than that predicted by (1). They attributed the faster phase speed to the effect of diabatic heating. Since if convective heating is assumed to be proportional to the vertical motion in the thermodynamic equation, the effect of diabatic heating on the propagation of VRWs can be considered in (1) by simply using a reduced static stability N^2 (Reasor and Montgomery 2001; Schechter and Montgomery 2007). This predicts a reduced retrograde propagation relative to the local tangential wind speed. As indicated in Wang (2002a), convection, thus the cyclonic PV generation, is generally enhanced immediately downwind of the maximum cyclonic PV anomaly in the eyewall. This favors a downwind shift of the maximum PV anomaly, implying a reduced retrograde azimuthal phase speed relative to the local tangential wind.

In addition to the transient asymmetric structure, quasi-stationary asymmetric structure may exist as a result of forced convective asymmetries. One of the examples is the convective asymmetries forced by environmental vertical wind shear. Wang and Holland (1996) showed that both upward motion and convection were enhanced to the downshear left of the TC center but suppressed to the upshear right when facing down shear. They attributed the development of convective asymmetries in the inner core region to the relative flow across the elevated cyclonic vorticity core. They also found a quasi-left tilt of the TC center with height and explained it as a result of circulation interac-

tions at different vertical levels. This distribution of asymmetry in eyewall convection due to vertical shear has been further studied by Frank and Ritchie (1999; 2001), Zhang and Kieu (2006) using more sophisticated high-resolution models and by Black et al. (2002) and Corbosiero and Molinari (2002, 2003) from observations and more recently by Heymsfield et al. (2006) as shown in Fig. 3 as an example.

The development of quasi-left tilted structure was then further studied theoretically by Reasor and Montgomery (2004), who considered an initially barotropic vortex embedded in a vertical shear on an f -plane. They proposed an inviscid damping mechanism intrinsic to the dry adiabatic dynamics of the TC vortex. By this mechanism, a vertically tilted vortex is considered to consist of an axisymmetric positive PV core surrounded by a skirt of lesser PV and a wavenumber-one baroclinic VRW projected by the tilted asymmetry. The subsequent damping of the wavenumber-one VRW in the presence of the PV skirt is regarded as the vertical alignment of the tilted vortex. This VRW damping mechanism provides a direct means of reducing the tilt of intense TC-like vortices in vertical shear. For initially upright, TC-like vortices in vertical shear, a “downshear-left” tilt equilibrium would be expected when the VRW damping is effective.

c. Spiral Rainbands

Spiral rainbands are distinct features of TCs. On one hand, they can produce severe weather; on the other hand, they may interact with the eyewall, causing TC structure and intensity changes in various ways (Barnes et al. 1983; Powell 1990a,b; Wang 2002b, 2009; Wang and Wu 2004; Nolan et al. 2007; Moon and Nolan 2010; Li and Wang 2012a,b). It is believed that the activity of spiral rainbands and their interaction with the eyewall convection as well as the storm scale circulation are key to the structure and intensity changes of TCs, such as the formation of concentric eyewall structure (see section 2d), size and size change (see section 2f), short-term intensity fluctuations (see section 3b). Therefore, it is important to understand the formation mechanisms and dynamical and thermodynamic structure and their interactions with the TC primary circulation.

Depending on their dynamics, origins, and radial extent, spiral rainbands within a radius of about 2-3 times of the RMW are generally referred to as inner spiral rainbands, while those farther outward are referred to as outer spiral rainbands (Wang 2009). Willoughby et al. (1984a) classified outer spiral rainbands into quasi-stationary rainbands and moving spiral rainbands. While the quasi-stationary outer spiral rainbands are mainly forced by quasi-steady forcing, such as vertical wind shear, the moving outer spiral rainbands could be triggered by different processes, such as inertial instability in the outflow layer, or variability of the core vorticity distribution, or interaction with neighbouring mesoscale convective systems, or their combination (Willoughby et al. 1984a; Guinn and Schubert 1993; Chow

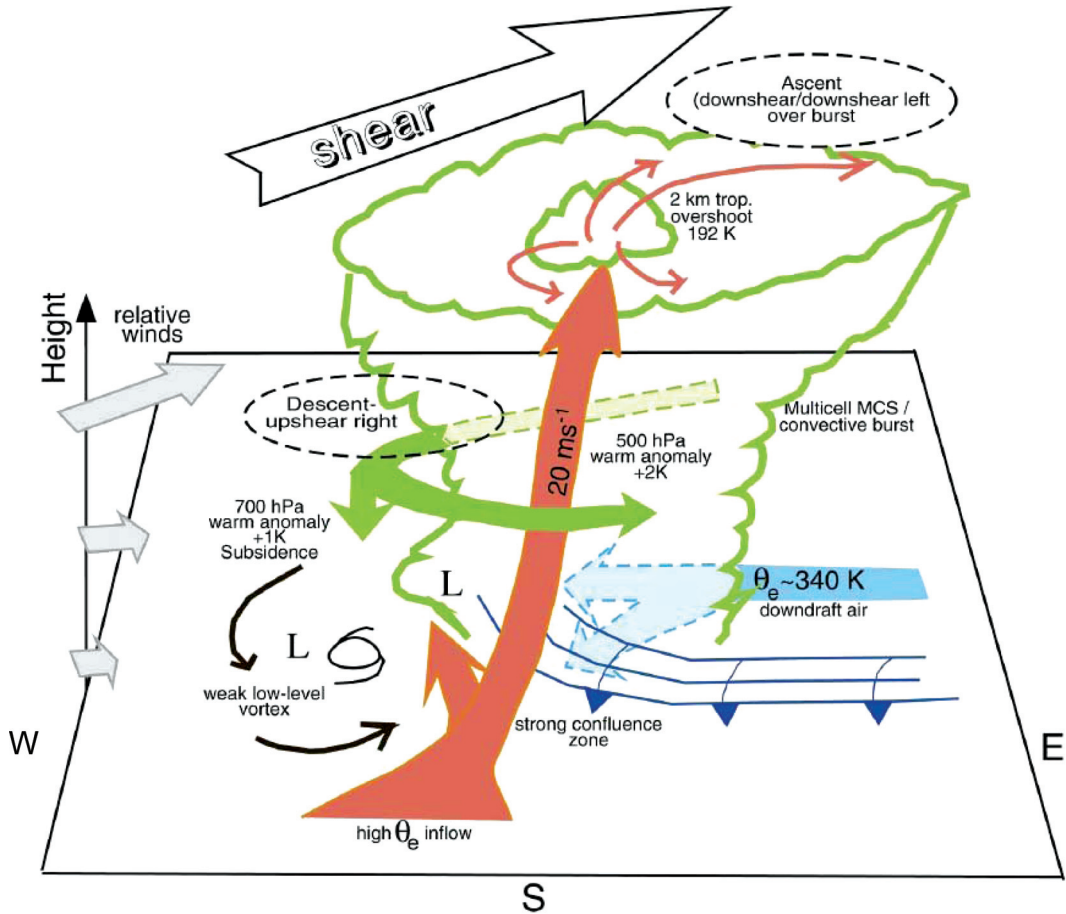


FIG. 3. Conceptual summary of Tropical Storm Chantal embedded in a vertical shear derived from aircraft and satellite observations, showing a poorly defined vortex that only extended from the surface up to mid-levels (LLC), and an adjacent intense convective region that comprised a mesoscale convective system (MCS) with extremely intense core about 10 km in diameter and peak updrafts exceeding 20 m s^{-1} . The relative easterly flow supporting the low-level convergence was highly modified by downdrafts and cold pool in the mid-lower troposphere from prior convection (adopted from Heymsfield et al. 2006).

et al. 2002; Schechter and Montgomery 2004, 2006; Li and Wang 2012a,b).

Since the annular region between the RMW and a radius of about 2-3 times the RMW is dominated by the strain flow in which the strain rate is larger than the relative vorticity, where the filamentation time is shorter than the convective overturning timescale, this annular region is termed the rapid filamentation zone by Rozoff et al. (2006). They suggested that all fields in the strain-dominated flow region are rapidly filamented and convection is hypothetically distorted and even suppressed, favoring the formation of the moat, an annular area immediately outside the eyewall as echo-free or weak echoes observed on radar images of a TC. In his full-physics model simulations, Wang (2008a) found that instead of suppressing deep convection, the rapid filamentation zone outside the RMW provides a

favorable environment for well-organized, sheared inner spiral rainbands. These inner spiral rainbands show characteristics, including their structure and propagation, closely related to the convectively coupled, sheared VRWs.

Outer spiral rainbands usually propagate radially outward (Kurihara 1976; Willoughby 1978; Chow et al. 2002; Wang 2009) and are generally characterized by extensive stratiform rainfall regions with embedded convective elements having varied degrees of organization (Barnes et al. 1983, 1991; Hence and Houze 2008; Li and Wang 2012a,b). Although earlier studies predominantly viewed outer spiral rainbands as inertia-gravity waves (Diercks and Anthes 1976; Kurihara 1976; Willoughby 1978), recent simulation and observational studies (Sawada and Iwasaki 2010; Yu and Tsai 2010; Li and Wang 2012a,b) suggest that outer spiral rainbands propagate radially outward with a much

slower speed than inertia-gravity waves and thus could not be attributed to the activity of inertia-gravity waves.

In a recent study, Li and Wang (2012a) analyzed the formation mechanisms of outer spiral rainbands in a simulated TC. They found that the outer spiral rainbands in their simulation are preferably initiated near the radius roughly about three times the RMW. After initiation, they generally propagate radially outward with a mean speed of $\sim 5 \text{ m s}^{-1}$. The outer rainbands are reinitiated quasi-periodically with a period between 22 h and 26 h in the simulation. They showed that outer spiral rainbands are triggered mainly by the inner rainband remnants immediately outside the rapid filamentation zone and inertial instability in the upper troposphere. The preferred radial location of initiation of outer spiral rainbands is understood as a balance between the suppression of deep convection by rapid filamentation and the favorable dynamical and thermodynamic conditions for initiation of deep convection.

The quasi-periodic occurrence of outer spiral rainbands is found to be associated with the boundary layer recovery from the effect of convective downdrafts and the consumption of convective available potential energy (CAPE) by convection in the previous outer spiral rainbands. Li and Wang (2012a) showed that once convection is initiated and organized in the form of outer spiral rainbands, it will produce strong downdrafts and consume CAPE, weakening convection near the location of its initiation. As the rainband propagates outward, the boundary layer air near the original location of convection initiation takes about 10 h to recover by extracting energy from the underlying ocean. Convection and thus new outer spiral rainbands will be reinitiated near a radius of about three times the RMW. This will be followed by a similar outward propagation and the subsequent boundary layer recovery, leading to a quasi-periodic occurrence of outer spiral rainbands. In response to the quasi-periodic appearance of outer spiral rainbands, the storm intensity experiences a similar quasi-periodic oscillation with its intensity starting to decrease after about 4 h of the initiation of an outer spiral rainband.

In another study, Li and Wang (2012b) compared the inner and outer spiral rainbands in their simulated TC. They further verified that the inner rainbands are characterized by the convectively coupled vortex Rossby waves. Convective cells in outer rainbands are typical of convective systems and move cyclonically and radially outward (inward) at large (small) radii. Convective cells in the upwind sector of the outer rainband tend to be clustered on the inner edge of the rainband, exhibiting more individual appearance. As the convective cells become mature, their high reflectivity cores move to the outer edge of the rainband and extensive stratiform precipitation occurs on the inner side of the middle sector of the rainband. Mature cells embedded in the outer rainband show a strong updraft coincident with the high reflectivity core and high θ_e , extending from near the surface to the upper troposphere. Net upward vertical mass

transports (VMTs) appear throughout the depth of the troposphere in the inner-rainband region, while net downward VMTs are found below 4 km height in the outer-rainband region. In the inner-rainband region, only a very shallow layer with net horizontal convergence appears below 2-km height, while a deep layer with net divergence aloft in the outer-rainband region. Strong upward motion prevails above 8-km height, while downdrafts and very weak subsidence predominate below in outer spiral rainbands.

d. Concentric eyewall structure

Concentric eyewalls often form in intense TCs (Hawkins and Helveston 2008; Kuo et al. 2009). The development of a concentric eyewall and the subsequent eyewall replacement (usually termed the concentric eyewall cycle) are one of the major mechanisms that can result in rapid TC structure and intensity changes (Willoughby et al. 1982; Houze et al. 2007; Stikowski et al. 2011). This phenomenon was first documented and studied in detail from observations by Willoughby et al. (1982). They showed that during some stages of intense TCs, spiral rainbands form a partial or complete ring of convection with heavy precipitation outside the eyewall of the TC. This convective ring usually possesses a well-defined local maximum tangential wind and a convergence in radial wind, very similar to the primary eyewall, and is thus generally called concentric or secondary eyewall. Because of the convergence of the boundary layer inflow into the secondary eyewall, the mass and moisture convergence into the inner, primary eyewall is reduced and convection in the inner eyewall weakens once an outer eyewall develops and intensifies. This is usually accompanied by a weakening of the storm and a contraction of the outer eyewall. Once the inner eyewall dies and is replaced by the outer eyewall, the storm could re-intensify if there are no unfavorable environmental conditions to occur.

Observational studies have revealed that concentric eyewalls only form in intense TCs and the associated intensity change varies considerably from case to case and the concentric eyewall structure can persist ranging from a few hours to more than a day (Hawkins and Helveston 2008; Kuo et al. 2009; Kossin and Sitkowski 2009). Based on 10-yr (1997–2006) satellite data, Hawkins and Helveston (2008) reported that about 80% TCs with a minimum central surface pressure lower than 940–950 hPa or the maximum surface wind greater than 50–60 m/s experience at least one concentric eyewall cycle in their life time over the western North Pacific while the ratio is reduced to 70% for the North Atlantic, 50% for the eastern Pacific, and 40% for the Southern Hemisphere. This indicates that in addition to the intensity, the particular regional environmental conditions could contribute to the formation of concentric eyewall structure as well. The intensity change in response to the eyewall replacement is found to be largely determined

by the nature of the heating in the secondary eyewall (Zhou and Wang 2011a). Large intensity oscillation is expected for those storms with stratiform heating dominated secondary eyewalls while small intensity change occurs in those with convective heating. Sitkowski et al. (2011) studied the inner-core structure and intensity changes associated with eyewall replacement cycles based on flight-level dataset consisting of 79 Atlantic basin hurricanes. They found that the mean locations of the inner and outer wind maximum at the time of formation of outer eyewall are at 35 and 106 km from the storm center, respectively, and the entire eyewall replacement cycle lasts 36 h on average. It is still unknown however what control the radial location of formation and the duration of the concentric eyewall. Based on idealized full-physics model simulation, Zhou and Wang (2011b) found that the ice-phase cloud microphysics may affect the radial location of the concentric eyewall formation and the subsequent intensity changes.

Several hypotheses have been proposed to explain the secondary (concentric) eyewall formation (SEF) although there have no any complete theories that can explain all aspects of the concentric eyewall cycle so far. Willoughby et al. (1982) proposed that symmetric instability at the bottom of the outflow layer could trigger the secondary convective ring and the SEF. Willoughby et al. (1984b) proposed that ice-phase cloud microphysics-related downdrafts may help initiate convective ring outside of the eyewall. They hypothesized that downdraft surrounding the eyewall brings down low momentum air, which induces a saddle in the wind profile, favorable for the formation of convergence at the outer edge of this saddle and thus the SEF.

Axisymmetrization of spiral rainbands is considered to be a plausible process causing the SEF (Willoughby et al. 1982; Black and Willoughby 1992). This was studied with a nondivergent barotropic model by Kuo et al. (2004, 2008), who simulated the concentric vorticity structure starting from a binary interaction of two vortices. Although the two-dimensional incompressible flow may not be appropriate for demonstrating the SEF mechanism (Moon et al. 2010), in idealized full-physics model simulations, Wang (2008a, 2009) confirmed that with the near-core moist environment axisymmetrization of outer spiral rainbands can lead to the SEF (see an example shown in Fig. 4). Similar mechanism is suggested to explain the SEF in Hurricane Rita (2005) by Judt and Chen (2010), who showed that the SEF in their numerical simulation resulted from the axisymmetrization of elevated PV generated and accumulated in spiral rainbands. Since the axisymmetrization of PV anomalies in spiral rainbands is effective in strong vortex, this mechanism can thus explain why concentric eyewall can only form in intense TCs.

Since the spiral rainbands can be triggered by either internal dynamics or external forcing, the rainband axisymmetrization mechanism suggests that the SEF could be either an internal process or triggered by external forcing.

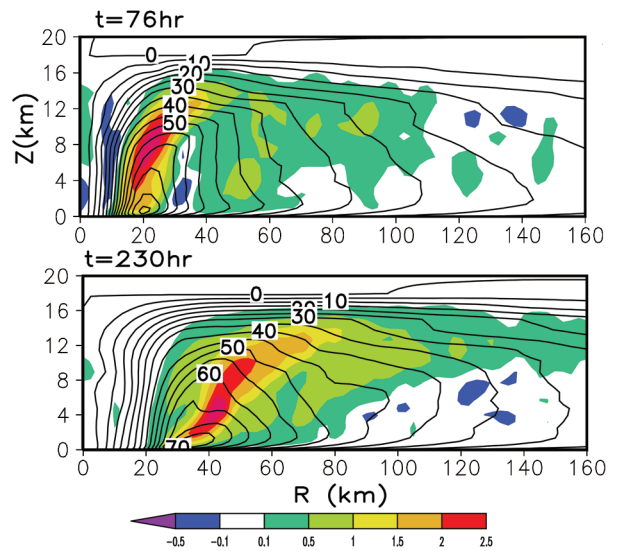


FIG. 4. Vertical-radial distribution of the azimuthal mean tangential wind speed in m s^{-1} (contours) and vertical velocity in m s^{-1} (shaded) at 76 h (a) and 230 h (b) of simulation showing the different vertical structures of a typical hurricane (upper panel) and an annular hurricane structure (lower panel) (from Wang 2008).

For example, Molinari and Vollaro (1990) suggested that the eddy angular momentum flux associated with an upper-tropospheric trough may initiate deep convection outside the eyewall and trigger major outer spiral rainbands and the SEF, as they showed in a case for Hurricane Elena (1985). A similar case was reported in a numerical simulation for Hurricane Bonnie (1998) by Zhu et al. (2004). The possible effect of upper level forcing on the SEF was also studied in an axisymmetric model by Nong and Emanuel (2003), who showed that cyclonic eddy angular momentum in the upper troposphere may be transported downward along the AAM surface to the surface and trigger local wind maximum outside the eyewall, which can enhance surface entropy flux and initiate deep convection, thus leading to the SEF.

Montgomery and Kallenbach (1997) proposed that the stagnation radius of outward energy dispersion of VRWs could be an ideal location for strongest wave-mean flow interaction and could trigger local wind maximum and thus the SEF. This possible mechanism was studied in a simple two-dimensional (2D) nondivergent barotropic model by Martinez et al. (2010). They showed that the axisymmetrization of vorticity perturbations outside a preexisting annular vortex with large vorticity skirt can induce a secondary wind maximum outside the primary eyewall. This secondary wind maximum was shown to result from the VRW-vortex-flow interaction, suggesting that VRWs could contribute to the secondary eyewall formation. Recently, studies with full-physics models have confirmed that VRWs do play important roles in the formation of concent-

tric eyewall (Qiu et al. 2010; Abarca and Corbosiero 2011; Martinez et al. 2011).

In addition to the wave-mean flow interaction, Terwey and Montgomery (2008) introduced a so-called “beta-skirt-axisymmetrization” (BSA) mechanism to explain their simulated SEF, which is based on the concept of two-dimensional (2D) turbulence theory. The 2D turbulence theory predicts an upscale cascade of eddy kinetic energy in the presence of the differential rotation (the so-called beta effect), namely the radial gradient of the azimuthal mean vorticity. By the BSA mechanism, in a region with a substantial overlap between the beta-skirt and an area of strong convective potential outside the eyewall, cumulus convective activity acts as a source of eddy vorticity and aids in the formation of the low-level jet by forcing additional low-level inflow into a narrow annular region with width determined by the so-called beta-scale. Upon coupling with the boundary layer via sensible and latent heat fluxes from the ocean surface, the induced jet can then amplify to enforce additional cumulus convection. This positive feedback and the continuous axisymmetrization lead to the SEF. This BSA differs from the VRW-mean flow interaction in that convective activity is not necessarily related to VRWs.

Both the wave-mean flow and the eddy-mean flow interaction mechanisms focus on asymmetric processes for the SEF. Actually, the possible role of axisymmetric dynamics in the SEF could not be excluded. In addition to the possible role of the outflow layer inertial or symmetric instability, an axisymmetric view has been proposed to explain the SEF in Typhoon Sinlaku (2008) by Huang et al. (2012). The secondary eyewall was shown to form after a sequence of structure changes in the outer core region starting from the broadening of the tangential winds above the inflow boundary layer, followed by an increase of the radial inflow in the boundary layer and supergradient winds in and just above the boundary layer, leading to an enhancement of convergence in the boundary layer where the secondary eyewall forms. However, it is unanswered what causes the broadening of tangential wind above the boundary layer and what determines the radial location of the boundary layer convergence and the SEF.

e. Annular Hurricane

Annular hurricanes have been identified as a new category of TCs by Knaff et al. (2003) based on infrared satellite images and aircraft reconnaissance data. Compared with the general population of TCs, an annular hurricane appears distinctly axisymmetric and has large circular eye region surrounded by a wide eyewall with a nearly uniform ring of deep convection and has no distinct spiral rainbands outside the eyewall. Knaff et al. (2003) found that the annular hurricanes have systematic formation characteristics, strong and steady intensities, and are observed in only specific environmental conditions. Once they form, the annular hurricanes can maintain their distinct structure and

intensity for several days if specific environmental conditions are maintained. The averaged intensity forecast errors for annular hurricanes were found to be 10–40% larger than for the typical hurricanes in the Atlantic and eastern Pacific during 1995–2001. Therefore, annular hurricanes pose a challenge to structure and intensity forecast (Knaff et al. 2003, 2008).

Based on infrared satellite images, Knaff et al. (2003) showed that the formation of annular hurricanes mainly results from asymmetric mixing of air between the eyewall and the eye, involving one or two mesovortices and culminating in the formation of quasi-axisymmetric storms with large eyes. They also found that the typical annular hurricanes form in very specific environmental conditions characterized by 1) weak easterly or southeasterly vertical wind shear, 2) easterly flow and relatively cold temperatures at 200 hPa, 3) a narrow range of sea surface temperatures (25.4° – 28.4° C) that are nearly constant, and 4) a lack of 200 hPa relative eddy flux divergence due to environmental interactions. The axisymmetric nature of annular hurricanes is speculated to be a result of the offset of internally-generated vertical northwesterly beta-shear by the weak vertical southeasterly environmental shear (Ritchie and Frank 2007). Although Knaff et al. (2003) revealed several aspects of the annular hurricanes, the use of satellite and aircraft reconnaissance data did not allow them to provide either the three dimensional dynamical and thermodynamic structure of the annular hurricanes or the detailed formation process and the maintenance dynamics.

In a fully compressible, nonhydrostatic TC model, Wang (2008b) simulated an annular hurricane which bears all observed characteristics of the annular hurricanes documented in Knaff et al. (2003). Although under idealized conditions, as observed, the simulated annular hurricane has a quasi-axisymmetric structure with wide eyewall, large eye and high intensity, and is lack of major spiral rainbands. Because the eyewall is wide, the elevated PV annulus in the eyewall generated by eyewall convection is also wide, giving rise to a barotropically less unstable structure of the axisymmetric vortex (Schubert et al. 1999). A striking feature of the simulated annular hurricane is its large outward tilt of the wide eyewall (Fig. 5), which is critical to the quasi-steady high intensity and responsible for the maintenance of the large-sized eye and eyewall of the storm. For such an annular storm, the strong massflux in the eyewall updraft corresponds to strong convective overturning flow, greatly suppressing the development of any major convective rainbands outside the eyewall. The formation of the annular hurricane in the simulation is found to be closely related to the interaction between inner spiral rainbands and the eyewall convection. Wang (2008b) showed that inner spiral rainbands may experience axisymmetrization due to strong shear deformation and rapid filamentation just outside the eyewall. As a result, the inner spiral rainbands become tightly wound and evolve into quasi-symmetric

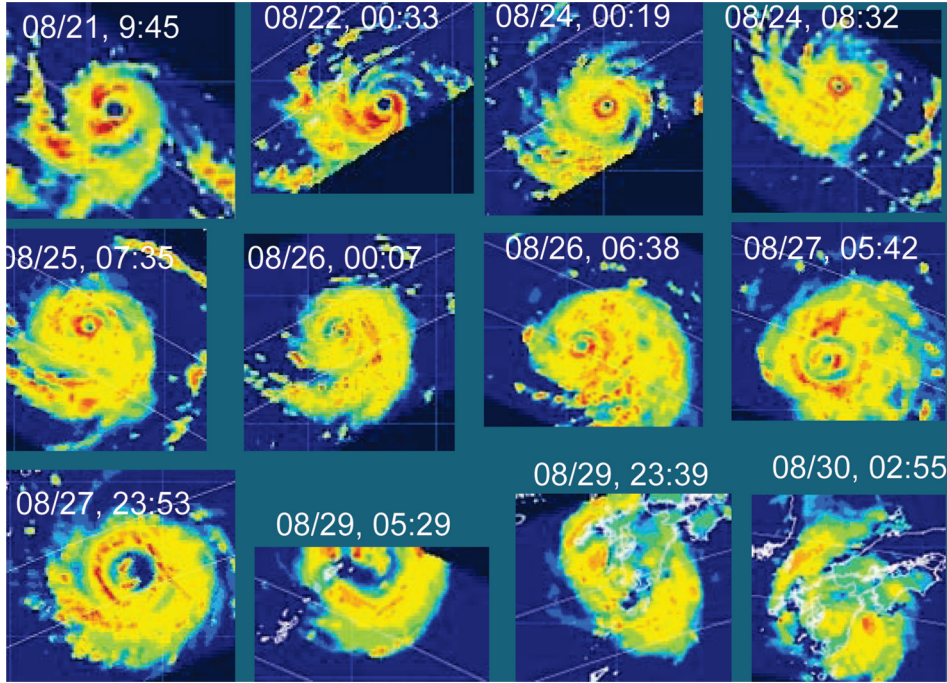


FIG. 5. Rain rate from TRMM satellite measurements for Supertyphoon Chaba (2004), showing the size change of the inner core related to the concentric eyewall cycles.

convective ring and propagates radially inward and intensifies while the eyewall breaks down and weakens. Eventually, the convective ring replaces the original eyewall. The new eyewall formed in such a way is wider and tilts more outward with height than the original eyewall. Several such eyewall cycles would eventually produce the annular hurricane with large eyewall slope, large eye, and wide eyewall.

This eyewall replacement process is very similar to the concentric eyewall cycle previously documented by Wilhoughby et al. (1982) and discussed in section 2d. The only difference is that no local maximum azimuthal mean tangential wind corresponds to the secondary convective ring in the annular hurricane formation in the simulation, which is one of the criteria for the SEF. This is mainly due to the fact that the secondary convective ring in the annular hurricane formation is too close to the eyewall to have its own local maximum tangential wind. Nevertheless, in a later study, Zhou and Wang (2009) reported that the annular hurricane can form as an end state of the classical concentric eyewall cycle.

f. TC Inner-core Size

The horizontal extent of damaging winds and torrential rain induced by a TC is not only determined by the TC intensity but also its size, in particular, its inner-core size. The TC size also affects the TC motion (e.g., Fiorino and Elsberry 1989; Fovell et al. 2009) and determines the

meridional transport of heat, moisture, and momentum, affecting the tropical-extratropical interactions and thus the atmospheric general circulation (Emanuel 2008). The TC size is also an important parameter for storm surge models and an important factor affecting the ocean upwelling under the TC (Price 1981; Irish et al. 2008). That is why the inner-core size and its change in a TC and the associated physical mechanisms have received increasing attentions in recent years (Wang 2009; Hill and Lackmann 2009; Xu and Wang 2010a,b).

The size of a TC can be measured in various ways. Among them the radii of the eye, maximum wind (RMW), gale force wind (17 m s^{-1}), damaging-force wind (25.7 m s^{-1}), hurricane-force wind (33 m s^{-1}), and the outmost closed isobar are frequently used in operational forecasts and statistical analyses (Merrill 1984; Weatherford and Gray 1988a,b; Kimball and Mulekar 2004; Moyer et al. 2007; Knaff et al. 2007; Maclay et al. 2008). Weatherford and Gray (1988a) defined the “inner-core” extending from the TC center to 1° latitude radius, while the “outer-core” being the region between radii of 1° and 2.5° latitudes. By their definition, the inner-core region of a strong TC generally includes the eye, RMW, and the radius of hurricane force wind. The outer-core region may cover the area with both the damaging-force winds and gale-force winds. Weatherford and Gray (1988b) showed that changes in the inner-core strength often occur independently from those in the outer-core strength. The former is closely related to the storm in-

tensity, while the latter seems to be affected greatly by the synoptic environmental conditions (Merrill 1984; Holland and Merrill 1984; Weatherford and Gray 1988b; Cocks and Gray 2002).

Observational studies show that the TC size varies with the season, region, latitude, environmental pressure, and even the time of the day (Kimball and Mulekar 2004; Moyer et al. 2007). Merrill (1984) found that on average TCs in the western North Pacific are twice as large as those in the Atlantic. Liu and Chan (2002) indicated that different TC sizes are associated with various synoptic flow patterns. The size of a TC also varies with time considerably. Macclay et al. (2008) examined the evolution of TC inner-core kinetic energy based on wind fields from aircraft reconnaissance flight level data. They found two processes that may lead to the growth of TC inner-core size, namely, the concentric eyewall cycle as discussed above (see Figs. 4 and 6 for examples) and the external forcing from the synoptic environment, such as vertical wind shear.

Wang (2009) emphasized the importance of latent heat release in outer spiral rainbands to the increase in the inner-core size of TCs. This led him to hypothesize that the TC inner-core size should be sensitive to the environmental relative humidity (RH), which can modify heating/cooling rate due to phase changes in outer spiral rainbands. He indicated that a deep moist layer in the near-core environment may favor the activity of strong outer spiral rainbands and thus the development of large TCs while a relatively dry environment may favor small, compact TCs. This possible effect was further studied by Hill and Lackmann (2009) based on a PV perspective. They showed that the diabatic generation of PV in spiral rainbands in the moisture-rich environment is critical to outward expansion of tangential wind fields and thus the increase in the TC inner-core size.

Although it has been established that energy required for the development and maintenance of a TC comes from the underlying ocean, it is not clear how the TC size may be affected by surface entropy flux at different radial regions.

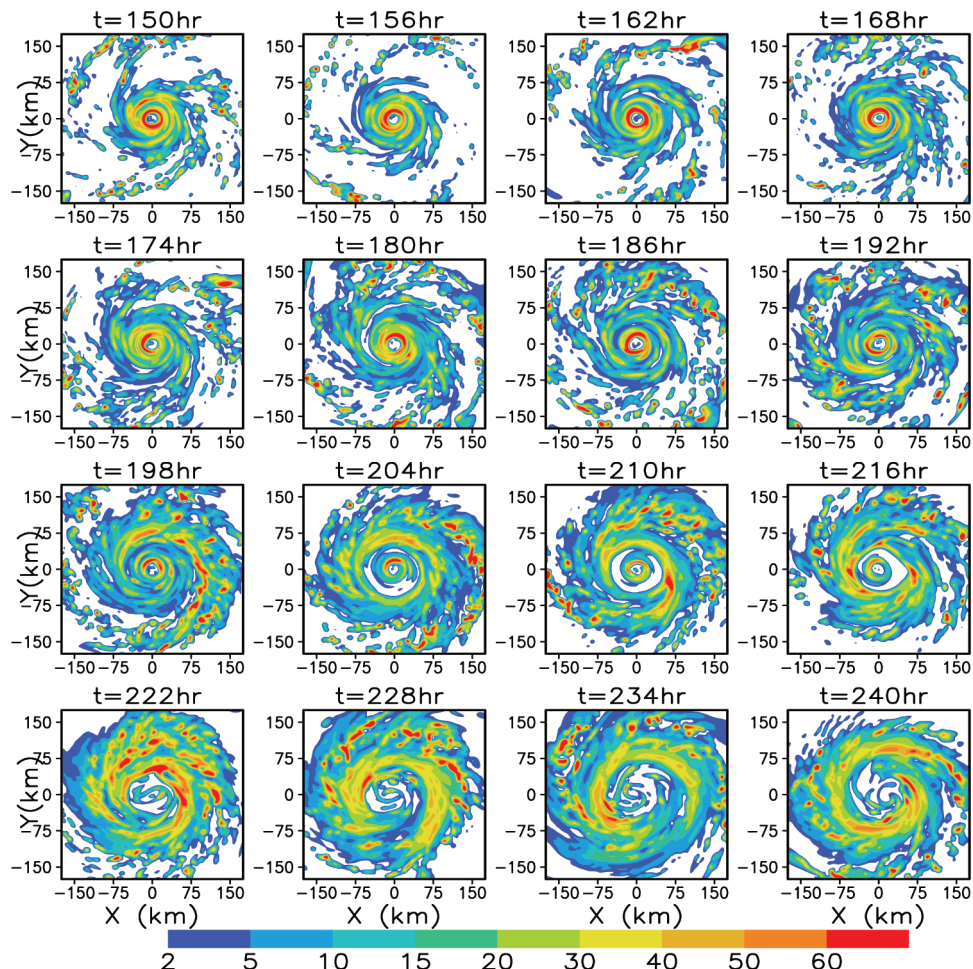


FIG. 6. 6-hourly surface rain rate (mm h^{-1}) 150 h to 240 h of simulation in an environment with 90% relative humidity, showing the concentric eyewall cycle in the TC model TCM4 as documented in Wang (2007).

This was studied by Xu and Wang (2010a) by artificially eliminating surface entropy flux in different radial extents in their idealized numerical simulations. They found that surface entropy flux outside the eyewall contributes largely to the activity of spiral rainbands and thus the increase in the TC inner-core size, in agreement with the hypothesis of Wang (2009) and the results of Hill and Lackmann (2009). These results thus may explain large TCs over the western North Pacific where RH in the summer monsoon environment is high, while relatively smaller TCs over the North Atlantic on average because of the effect of dry Saharan Air Layer (SAL, Dunion and Velden, 2004; Wu et al. 2006; Wu 2007; Shu and Wu 2009), and even smaller TCs over the central Pacific where the trade wind region is dominated by dry conditions in the middle troposphere (Wang 2009).

Cocks and Gray (2002) found that small TCs were smaller than the medium and large TCs early on and throughout their respective lifetimes. The physical mechanism responsible for this tendency was recently studied by Xu and Wang (2010b) based on idealized simulations. They identified a positive feedback between the outward expansion of tangential wind field, which causes large surface entropy flux outside the eyewall, and the activity of spiral rainbands. Specifically, a large initial size vortex has a broad tangential wind distribution outside the RMW, causing large surface entropy flux outside the eyewall and favoring the development of active spiral rainbands. Diabatic heating in spiral rainbands drives strong inflow in both middle troposphere and in the boundary layer outside the eyewall (Fudeyasu and Wang 2011), bringing high AAM inward and increasing tangential winds outside the eyewall, leading to the outward expansion of the wind field and the increase in the inner-core size of the TC. This is a positive feedback for the large initial size vortex to steadily increase its inner-core size (see a similar effect of the initial wind profile outside the RMW discussed by Stern and Nolan 2011). On the contrary, a small initial size vortex has weak winds and thus small surface entropy fluxes outside the eyewall, prohibiting the development of active spiral rainbands in large radii, resulting in much weak inflow outside the eyewall in the mid-lower troposphere and limiting the radial advection of AAM. As a result, the increase in tangential winds outside the eyewall and thus the outward expansion of the wind field are prohibited, thus the inner-core size remains small. Xu and Wang (2010b) also found that the inner-core size of the simulated storm at the mature stage depends more greatly on the initial vortex size than on the initial RH of the environment. Since most of TCs form from relatively large-scale disturbances in the monsoon trough over the western North Pacific while from easterly waves, which have small scale features near the surface, over the Atlantic, the results of Xu and Wang (2010b) suggest that the mean storm size should be larger over the western North Pacific than over the North Atlantic, consistent with observations (Merrill 1984).

3. Tropical Cyclone Intensity

As a step toward understanding the TC intensity and intensity change, attempts have been made to estimate an upper bound of TC intensity for given atmospheric and oceanic environmental conditions. Such an upper bound is called the maximum potential intensity (MPI) of a TC. In this section we will provide a literature review on our current understanding of the MPI theories and their limitations. Although theoretically there exists an MPI for each TC in a given favorable environment conditions, no one of the available theories are complete due to different assumptions or approximations of the complicated physical and dynamical processes. Nevertheless, in reality, few TCs can reach their MPIs because of many environmental factors and/or internal processes that limit the TC intensity. Therefore, understanding what limits the TC intensity is equally important to understanding what determines the MPI of a TC. We thus will focus on these two aspects in this section.

a. The Maximum Potential Intensity (MPI)

The current available MPI theories can be roughly classified into two categories: one assumes that as a TC intensifies the frictional dissipation increases and eventually limits the TC intensification, and thus an upper bound of the TC intensity exists (Emanuel 1986; 1988, 1991, 1995) and the other one assumes that the energy provided by the ocean and the environment could not be used infinitively by the TC system and thus there is an upper bound to stop the TC further intensifying (Holland 1997). Since the latter does not explicitly include the energy dissipation of the TC system and it also needs a parameterized TC eye while it lacks any eyewall size parameter, restrictedly speaking, it is not a complete theory (Camp and Montgomery 2001). We will thus only focus on the Emanuel's MPI theory (E-MPI hereafter) below.

There are two derivations of the E-MPI: E-MPI1 (Emanuel 1986, 1988, 1991, 1995; Bister and Emanuel 1998) and E-MPI2 (Emanuel 1997). E-MPI1 is based on the assumption that the TC behaves like a classic Carnot heat engine in which energy is added at the underlying warm ocean and lost in the cool outflow layer. An array of assumptions were made to derive a relationship between the central pressure and environmental parameters, including axisymmetric structure, both hydrostatic and gradient wind balances, slantwise moist-neutral condition, etc. Therefore, the MPI measured by the minimum central surface pressure of a TC can be determined entirely by the cyclone radius at which environmental parameters of sea-level pressure, SST, and RH, and the air temperature of the outflow layer in the upper troposphere are defined. Since the available energy for a TC in E-MPI1 is determined by the maximum entropy difference between the cyclone eyewall and the environment, the E-MPI1 is markedly sensitive to the choice of environmental parameters, such as the environmental RH

(Holland 1997; Camp and Montgomery 2001).

By incorporating eye dynamics, which is closed by assuming a balance between the radial entropy advection and the surface entropy flux together with an assumption of cyclostrophic balance, Emanuel (1995) modified his original E-MPI1. This revised E-MPI1 shows an explicit dependence of the MPI measured by the maximum azimuthal mean surface wind speed on the ratio of the exchange coefficient to the drag coefficient at the air-sea interface and showed a better agreement with the numerical model results. The E-MPI1 was further elaborated by incorporating the effect of dissipative heating in the boundary layer, producing an MPI measured in maximum surface wind speed about 22% higher (Bister and Emanuel 1998).

The second derivation of the Emanuel's theoretical MPI, E-MPI2, is a simplification of his earlier analytical MPI. Emanuel (1997) assumed that when the storm reached its MPI, the rate of energy input from the ocean surface should be approximately balanced by the surface frictional/mechanical dissipation to the ocean. Considering the efficiency of the Carnot engine, the net energy input thus can be written as

$$\text{Energy}_{\text{input}} = \int \frac{T_s}{T_{\text{out}}} \varepsilon C_k \rho |\vec{V}| (k_o^* - k_a) r dr \quad (2)$$

where C_k is the enthalpy transfer coefficient at the ocean surface, k_o^* is the saturation enthalpy at the sea surface temperature (T_s), k_a is the enthalpy of the air in the well-mixed boundary layer, $|\vec{V}|$ is the total near-surface wind speed, ρ is the air density, and

$$\varepsilon = \frac{T_s - T_{\text{out}}}{T_s} \quad (3)$$

is the thermodynamic efficiency of the Carnot heat engine, where T_{out} is the outflow-layer temperature. Note that the dissipative heating is included in (2). Without dissipative heating, the factor T_s/T_{out} will become 1.0 (Bister and Emanuel 1998). The mechanical energy loss to the underlying ocean from the system can be expressed as

$$\text{Dissipation} = \int C_D \rho |\vec{V}|^3 r dr \quad (4)$$

We can see that the energy input increases with wind speed linearly while the energy dissipation increases with wind speed cubically. This implies that as the storm intensifies, both the energy dissipation and the energy input increase while the former increases faster than the latter. At a stage when the energy dissipation reaches the energy input, the TC could not intensify any more, namely the TC reaches its MPI (as schematically shown in Fig. 7). Theoretically, this balance is reached for the whole TC system at the maximum intensity. Since both terms are dominated by the winds under the eyewall, Emanuel (1997) thus assumed that the balance can be evaluated under the RMW. As a result, the MPI (V_m) can be approximated by

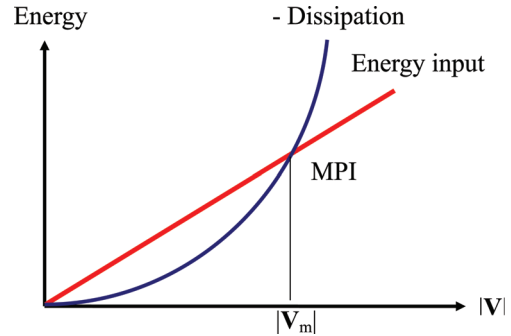


FIG. 7. Schematic of changes of energy dissipation (blue) and energy input (red) with wind speed in a typical tropical cyclone.

$$V_m = \sqrt{\frac{T_s}{T_{\text{out}}} \frac{C_k}{C_D} \varepsilon (k_o^* - k_a)} \quad (5)$$

Emanuel (1997) indicated that although E-MPI2 (5) was derived as an approximation, it has the same form as an expression for EMPI1, which was derived analytically from the entropy balance of the subcloud layer in the eyewall with the assumption that entropy is constant along the angular momentum surfaces.

Although earlier numerical results from axisymmetric TC models demonstrated that the E-MPI can give an excellent estimation of the modeled TC maximum intensity (Rotunno and Emanuel 1987; Emanuel 1995, 1997), later studies show that numerically simulated TC maximum intensity can exceed the E-MPI when very high-resolution models are used (Persing and Montgomery 2003; Cram et al. 2007; Yang et al. 2008; Bryan and Rotunno 2009a). These high-resolution model results are supported by recent observational studies (Montgomery et al. 2006; Bell and Montgomery 2008). In fact, the intensities of both modeled and observed TCs can be higher than the E-MPI by as much as 10–50%. Such a phenomenon was termed superintensity by Persing and Montgomery (2003). They hypothesized that the near-surface high entropy air in the eye region could serve as an additional source of energy for the TC heat engine if the air is entrained into the eyewall, an effect is not included in the E-MPI theory, and thus considerably increase the TC intensity (Cram et al. 2007).

The above hypothesis was evaluated by Bryan and Rotunno (2009a) using a very high-resolution axisymmetric TC model. They found that less than 3% of the total entropy input to the TC could be attributed to the air from the eye because of the relatively small volume of the eye. As a result, the total magnitude of entropy transport from the eye to the eyewall was negligible in the entropy budget and contributed less than 4% to the simulated TC intensity, suggesting that high-energy air in the boundary layer in the eye is unlikely a major factor for the superintensity as hypothesized by Persing and Montgomery (2003). The ap-

proximation of the energy balance under the eyewall made by Emanuel (1997) was later evaluated in a numerically simulated TC by Wang and Xu (2010). Wang and Xu (2010) found that the energy input and energy dissipation do not balance under the eyewall. They showed that the inward transport of energy in the inflow boundary layer into the eyewall contributes significantly to the entropy budget in the eyewall and thus a considerable portion of the TC superintensity.

Smith et al. (2008) suggested that the assumption of gradient wind balance in the boundary layer is a major shortcoming of the E-MPI theory and is responsible for the systematic underestimation of the TC MPI. They suggested the use of a more complete dynamic boundary layer model in E-MPI. In a recent study, Bryan and Rotunno (2009b) presented an analytic diagnostic model including the radial momentum budget in the boundary layer and demonstrated that the imbalanced flow in the boundary layer could contribute considerably to the TC maximum intensity. These two studies focused on the deficiency in the dynamical aspect of the E-MPI. Since the inflow boundary layer is largely driven by the agradient wind and determines the inward energy transport as identified by Wang and Xu (2010), the results of Smith et al. (2008), Bryan and Rotunno (2009b) and Wang and Xu (2010) therefore all reveal the same shortcomings of the assumption made for the gradient balance in the inflow boundary layer when the E-MPI is derived.

In addition to the contribution of the imbalanced flow, in a latest study, Frisia and Schönenmann (2012) relaxed the assumption of the neutral conditions of slantwise convection and developed an extended model including the eye dynamics for the E-MPI. Their revised model predicts TC intensity exceeding the E-MPI, suggesting that convective potential energy (CAPE) outside the eyewall contributes to the TC maximum intensity. This provides another possible mechanism for the superintensity in both model simulations and observations. This is consistent with the results of Wang and Xu (2010) that energy input from outside of the eyewall can explain a large portion of the superintensity.

In addition to the boundary layer processes, Emanuel and Rotunno (2011) further relaxed the assumption of a constant outflow layer temperature which is determined by the far-field environment in the original E-MPI. Motivated by the convection-resolving axisymmetric model simulations, Emanuel and Rotunno (2011) proposed a self-stratification process in the TC outflow layer. By this mechanism, the entropy stratification in the outflow layer is set by small-scale turbulence that limits the Richardson number and thus it is determined by a requirement that the Richardson number not below a critical value. This allows them to derive an equation for the variation of outflow layer temperature with the AAM surface, leading to a new prediction of the structure and intensity for a steady-state TC. Since the maximum intensity based on this new assumption for $C_k/C_D > 1$ (< 1) is lower (higher) than the original E-MPI, it could not

explain the superintensity phenomenon. Nevertheless, this new outflow layer temperature allows Emanuel (2012) to examine the intensification process of a TC. These results also suggest a need to pay attention to the outflow layer processes in TCs.

b. Factors limiting TC intensity

Although the E-MPI considerably underestimates the MPI of a TC, observations still show that on average only a small portion of TCs can reach 20% of their theoretical E-MPI or the SST-determined MPI (DeMaria and Kaplan 1994; Zeng et al. 2007, 2008). This indicates that there are factors that limit TC intensity in reality (Camp and Montgomery 2001; Emanuel et al. 2004). Understanding those factors can help improve the intensity forecasts of TCs. Here we will focus on several factors that are extensively studied in recent years.

1) Internal dynamics

There are various internal processes that may limit TC intensity. The mostly-cited process is the SEF as discussed in section 2d. In addition to the SEF, the internally-generated asymmetric structure in the eyewall, such as VRWs as discussed in section 2b, was found to reduce the azimuthal mean winds near the RMW, limiting the TC intensity as demonstrated in Yang et al. (2007). In addition to the asymmetric structure in the eyewall, spiral rainbands may also limit the TC intensity through broadening the tangential wind outside the eyewall, reducing the moisture and mass convergence into the eyewall, and thus reducing the TC intensity as recently studied extensively based on idealized simulations (Wang 2009; Li and Wang 2012a, b).

2) Translational speed

The maximum intensity of a TC may be affected considerably by its own translational speed, which in turn is determined by the deep layer mean environmental flow plus a so-called beta-drift. Indeed, earlier observational studies showed that the TC intensity and their translation speed are highly correlated (Wang and Wu 2004; Zeng et al. 2007, 2008, 2010). As shown in Zeng et al. (2007, 2008), the very intense TCs are those with translation speeds between 3 and 6 m s⁻¹ in both the western North Pacific and the North Atlantic.

The lack of very intense storms with slow translational speeds results mainly from the oceanic cooling induced by the vertical mixing in the upper ocean forced by surface wind stress curl, which may disrupt the further intensification of very intense TCs. Such a relationship was recently examined by Mei et al. (2012) based on 40-year TC best track data. Their composite analysis provides evidence that the translational speed of a TC can exert a significant control on the TC intensity by modulating the strength of the negative effect of the storm-induced oceanic cooling on TC intensification. They showed that storm intensity correlates

with translational speed, with TCs of category 5 moving on average 1 m s^{-1} faster than tropical storms in the tropics.

Translational speed can also introduce asymmetric surface heat and moisture fluxes and friction to a TC, generating the asymmetric structure in the inner core region (Shapiro 1983; Kepert and Wang 2001). As a result, if a TC moves too fast the resulting asymmetric structure would inhibit intensification as shown by Peng et al. (1999). In their numerical experiments, Peng et al. (1999) found a reduction of the intensity for a TC embedded in a uniform environmental flow. They showed that the relative phasing of asymmetric surface fluxes and moisture convergence in the boundary layer was responsible for the intensity reduction. The effect of superimposed uniform environmental flow on the TC intensity can also be explained by the energy balance in the TC system. Specifically, if everything else is axisymmetric about the storm center while a uniform environmental flow is added to the total wind and an azimuthal integration is performed, one can find that the uniform flow does not affect the energy input shown in (2) but it contributes a positive value to the energy dissipation in (4). This implies that part of the energy input would be used to balance the extra energy dissipation due to the imposition of a uniform environmental flow or equivalently the translational speed of a TC.

3) Vertical shear

Vertical shear of horizontal wind is considered a major limiting factor to the intensification and intensity of TCs. A common explanation of the effect of vertical wind shear is the “ventilation” of the warm core (Gray, 1968). Observational studies show that overall, vertical shear, in particular, the shear in the upper troposphere, is negative to TC intensification (DeMaria and Kaplan 1994; Emanuel 2000; Patterson et al. 2005; Zeng 2007, 2008, 2010) although some intense TCs can still survive in vertical shear as large as 20 m s^{-1} over the western North Pacific and the North Atlantic (Zeng et al. 2007, 2008). Zeng et al. (2008) also introduced a dynamical efficiency to the empirical SST-determined MPI, which takes into account the combined negative effect of both translational speed and environmental vertical shear.

Frank and Ritchie (2001) attributed the weakening of the TC in their simulation to the outward eddy flux of high values of PV and equivalent potential temperature by the vertical shear-induced asymmetry in the upper troposphere, resulting in the weakening of the warm core at the upper levels. This mechanism does not need evident vertical tilt of the TC while emphasized an upper-down weakening process of TCs embedded in vertical shear. Because of the upper-level origin and the thermodynamic nature, the ventilation of warm core either by the advection of the sheared environmental flow or by the shear-induced asymmetric eddies can be considered as the “upper-level ventilation”.

In a recent study, Riemer et al. (2010) emphasized the

effect of convective downdraft-induced low-entropy air in the inflow boundary layer. The inward transport of the low-entropy air by the radial inflow to the inner core may suppress eyewall convection, and limiting the TC intensity. This process can be considered as the “low-level ventilation” because the effect is through the low-level inflow although the original low-entropy air is from the mid-troposphere enhanced by vertical shear. Indeed this has been also used to explain how the convective downdrafts in outer spiral rainbands may affect the eyewall convection and TC intensity by Powell (1990a,b), Black et al. (2002), Li and Wang (2012a).

In addition to the upper-level and low-level ventilation effects, dry, low-entropy air in the mid-troposphere outside of the eyewall may be directly fluxed into the eyewall by the shear-induced eddies and dilute the high-entropy air in the eyewall, limiting the TC intensity (Cram et al. 2007). This can be referred to as the “mid-level ventilation”. Emanuel (2004) included this effect by introducing an extra term into the mid-level thermodynamic equation representing the negative ventilation effect of environmental vertical shear. In a later study, Tang and Emanuel (2010) introduced this effect into the idealized Carnot heat engine of E-MPI theory and showed that the mid-level ventilation has a detrimental effect on the TC maximum intensity. In particular they found that there exists an upper-ventilation bound beyond which no steady TC can exist. This mid-level ventilation is also shown to decrease the thermodynamic efficiency as the eyewall becomes less buoyant relative to the storm’s environment.

In addition to the three thermodynamic effects, vertical shear can reduce the TC intensity through dynamical processes, such as the development of vertical tilt of the TC inner-core structure (DeMaria 1996; Wong and Chan 2004) and the development of convective asymmetries (Wang and Holland 1996; Wu and Braun 2004). Dynamically, the vertical shear-induced convective asymmetries in the inner core region can result in eddy momentum fluxes, which reduce the azimuthal mean tangential wind near the RMW, and thus limiting the TC intensity (Wu and Braun 2004).

4) Other factors

There are still many other factors that may limit TC intensity. Ocean upwelling as mentioned earlier is one of them. This oceanic feedback is well known and its effect on TC intensity is determined by several important factors, such as the translational speed, size, and intensity of the TC, as well as the ocean mixed layer depth (Shade and Emanuel 1999; Chan et al. 2001; Zhu et al. 2004; Wu et al. 2007). Since the theoretical MPI does not include the ocean negative feedback, the observed TC intensity is often less than the MPI.

Another important factor is whether a TC has enough time to intensify after its formation over the warm tropical ocean. If a TC forms not too far away for the land mass, the

TC could not have enough time to intensify to its MPI. For examine, over the western North Pacific, TCs formed in the eastern part of the basin usually have longer time to move over the warm ocean and on average get higher intensity than those formed in the western part of the basin, such as in the El Nino developing year (e.g., Wang and Chan 2002; Zhan et al. 2011). Another possible factor limiting TC intensity is the so-called dry-air intrusion, which describes the process that the continental air intrudes the TC inner core region when a TC approaches the large landmass (e.g., Lowag et al. 2008; Sun et al. 2009).

Islands over the ocean on the path of a TC may affect the TC structure and intensity significantly. Even the island has a scale comparable to the eyewall size, it may insert a considerable impact on TC structure and intensity changes. One such example is the trigger of the SEF as discussed by Black and Willoughby (1992). In this case, islands orography may lead to the asymmetric structure and trigger the formation of strong spiral rainbands, which may evolve into a concentric eyewall (see section 2d). Another effect of island topography is the possibility to result in the eyewall breakdown, and thus interrupting the intensification of the TC, such as TCs passing Luzon Island of the Philippines over the western North Pacific studied by Brand and Bleloch (1973), Wu et al. (2003), and Chou et al. 2011).

4. Some Remaining Issues and Future Research Directions

Although significant progress has been made in understanding the TC structure and intensity, there are still a lot of issues that need to be addressed in future studies. Here only some personal views will be briefly discussed. Hopefully the issues identified below may be addressed by the research community in the near future.

a. What determines the size of the RMW?

Although we know that there exists an RMW for any TC, it is still a puzzle so far what exactly determines the size of the RMW. Theoretically, in a given low pressure system, any parcel initially far away from the RMW in the inflow boundary layer that spirals cyclonically inward to the TC center should not reach the center of the storm because of the increasing centrifugal force which is inversely proportional to the square of the radius. Since the AAM is lost to the surface in the inflow boundary layer, it is difficult to determine the radius at which the parcel's centrifugal force would balance the radial pressure gradient force plus the deceleration of the radial wind. Given the pressure distribution, the time-dependent solution for the parcel will be determined by the outer radius at which the radial pressure gradient diminishes and the surface friction. The outer radius may be initially determined by the size of the initial TC disturbance while late on may be considerably affected by the forced secondary circulation due to the internal atmospheric diabatic heating in both the eyewall and active

spiral rainbands as recently examined by Xu and Wang (2010b). Emanuel and Rotunno (2011) derived an expression of the RMW for a steady-state TC, which includes the outer radius mentioned above and also the MPI. Nevertheless, a detailed close examination of this issue is still needed to give a complete picture.

b. What determines the outer-core wind structure?

Winds outside the RMW generally decay with radius, while different rate may occur to different storms or to the same storm at different stages of its lifetime. It is still a puzzle what determines the decaying rate of tangential wind with radius outside the eyewall. Earlier studies (e.g., Holland and Merrill 1984) demonstrated the possible role of the environmental eddy momentum flux forcing in the upper troposphere in the TC outer-core size increase. Several recent studies have revealed that diabatic heating outside the eyewall associated with active spiral rainbands plays critical role in driving the secondary circulation and the spin-up of the tangential winds outside of the eyewall (Wang 2009; Xu and Wang 2010a,b; Fudeyasu and Wang 2011). However, these studies have focused mainly on the internal dynamics, such as the near-core environmental RH, the wind profile of the pre-TC vortices, it is still unclear how the horizontal and vertical shears in the environmental flow may trigger the development of spiral rainbands and thus the TC outer-core wind profile in addition to the upper tropospheric inward angular momentum fluxes. Therefore observational and numerical studies could be performed to examine the relationship between the activity of spiral rainbands with different environmental flow patterns and the associated storm outer-core wind evolution.

c. What determines the outward slope of the eyewall?

Although recent studies have demonstrated that the outward slope of the eyewall with height increases with the size increase of the eyewall itself (Stern and Nolan 2009), mainly following the AAM surface. This is consistent with the decrease of the tangential wind with height due to the warm core structure of a TC. However the rate of the decrease of tangential wind with height is determined by the radial temperature gradient across the eyewall. It is not clear what determines the height of the warm core and what determines the radial extent of the warm core, both are critical to the outward slope of the azimuthal mean AAM surface. Therefore future studies may focus on understanding the formation, vertical structure, and horizontal extent of the warm core of a TC and their relationship to the outward slope of the AAM surface.

It is not clear whether the height of the warm core is related to the outward slope of the eyewall or the size of the eyewall. By the argument of thermal wind balance, if the eyewall occurs at a relatively large radius and has a large outward slope in the mid-lower troposphere, the tangential wind would decrease with height rapidly. This will imply

a large radial temperature gradient in the mid-lower troposphere, or equivalently a warm core in the middle troposphere. In contrast, if the eyewall occurs in a small radius and has small outward tilt in the mid-lower troposphere, the warm core would be expected to occur in the upper troposphere. However, in a recent study by Stern and Nolan (2012), they found that the height of the warm core might have nothing to do with the thermal wind balance. In their idealized simulations, the warm core was often found in the layer between 4 and 8 km heights, while a secondary, weaker warm core may be found near 13–14 km height. This is in contrast to the typical upper-tropospheric (>10 km) warm core previously believed. Since the results of Stern and Nolan (2012) were obtained from one model with specified conditions, studies with different models and with a wide range of parameter space in model settings should be conducted to clarify this issue.

d. Concentric eyewall cycle

Although several plausible mechanisms have been proposed to explain the SEF, they are quite diverse. Some of them are complementary while some others are inconsistent. They can be roughly classified into three groups: asymmetric versus axisymmetric dynamics, convection first versus the secondary wind maximum first, and a top-down process versus a bottom-up process. The diversity suggests that the concentric eyewall may form from one mechanism in one TC while from different mechanisms in different TCs. This further demonstrates that the dynamics of the SEF is far from being sufficiently understood. It is further complicated by the involved cloud microphysical processes.

There have been no complete theories that can explain all aspects of the concentric eyewall cycle so far. In particular, little attention has been paid to explain where and when the secondary eyewall will form and after their formation how long it can maintain and eventually replaces the primary eyewall and how much intensity change would be expected for a given case. These all are important to TC structure and intensity forecasts.

e. Complete MPI theory

The MPI concept is fundamental to our understanding of TC intensity although only a small portion of TCs that can reach their theoretical MPI. However, as we discussed in section 3a, the current MPI theories are incomplete. It is expected that more realistic assumptions can be used in deriving the MPI. Dynamically, it might be important to consider how the effect of the unbalanced flow in the boundary layer can be included. From viewpoint of energetics, it is necessary to consider the energy input in the inflow boundary layer from outside of the eyewall. The existence of slantwise CAPE outside the eyewall could be another source of superintensity, which has been recently proposed (Frisius and Schönenmann 2012). Furthermore, recent at-

tention has also been given to the processes in the outflow layer (Emanuel and Rotunno 2011; Emanuel 2012). It is expected that a more complete MPI theory may emerge after some extended efforts in the near future.

f. Effect of vertical shear

Although the effect of vertical shear on TC structure and intensity has been extensively studied in the past, it is still one of the least understood aspects in TC dynamics. Dynamically, vertical shear affects TC structure and intensity through quasi-steady asymmetric forcing that may reduce the capability for axisymmetrization of the TC circulation, thus limiting the TC intensification and intensity. Previous studies have already shown that large size TCs are less affected by vertical shear, indicating that the axisymmetrization potential and vertical alignment of the sheared TC may strongly depend on the size and strength of the TC itself. However, the measure of such a potential needs to be investigated and quantified. The rich phenomena, such as the forced active spiral rainbands, the concentric eyewall cycle, and size increase, resulting from the interaction between a mature TC and an imposed easterly vertical shear, currently being studied by the author's group are shown in Fig. 8.

Furthermore, the response of both TC intensity and structure to vertical shear may depend on the vertical profile of the shear, as mentioned in section 3b. Observational studies have revealed that the response of TC structure and intensity changes to the upper-level shear could be quite different from that to the lower-level shear. The involved physical mechanisms, however, need to be investigated further. Possible factors may include the static stability, inertial stability, and the strength of the warm core of the TC, all these change drastically with height. The amplitude of the asymmetric structure forced by vertical shear may depend strongly on the vertical profile of the shear. Such dependency would further affect the TC structure and intensity through nonlinear interactions between the symmetric circulation and the asymmetric structure. In addition, although three thermodynamic ventilation effects have been identified, their relative importance and the relative importance of the dynamical and thermodynamic effects are yet not clear and should be addressed in future studies as well.

g. Stratosphere-troposphere exchange (STE)

Another topic related to TC structure and intensity and their changes is the stratosphere-troposphere exchange (STE). Some studies have observed the injection of tropospheric air into the lower stratosphere near the eyewall of TCs, which can be revealed by the low ozone concentration, based on satellite data, aircraft measurements and in-situ observations (e.g., Penn 1966; Danielsen 1993; Romps and Kuang, 2009). These studies attributed the upward transport across the tropopause to the rapid overshooting convection and internal gravity waves induced by vertical velocity difference. On the other hand, some studies have

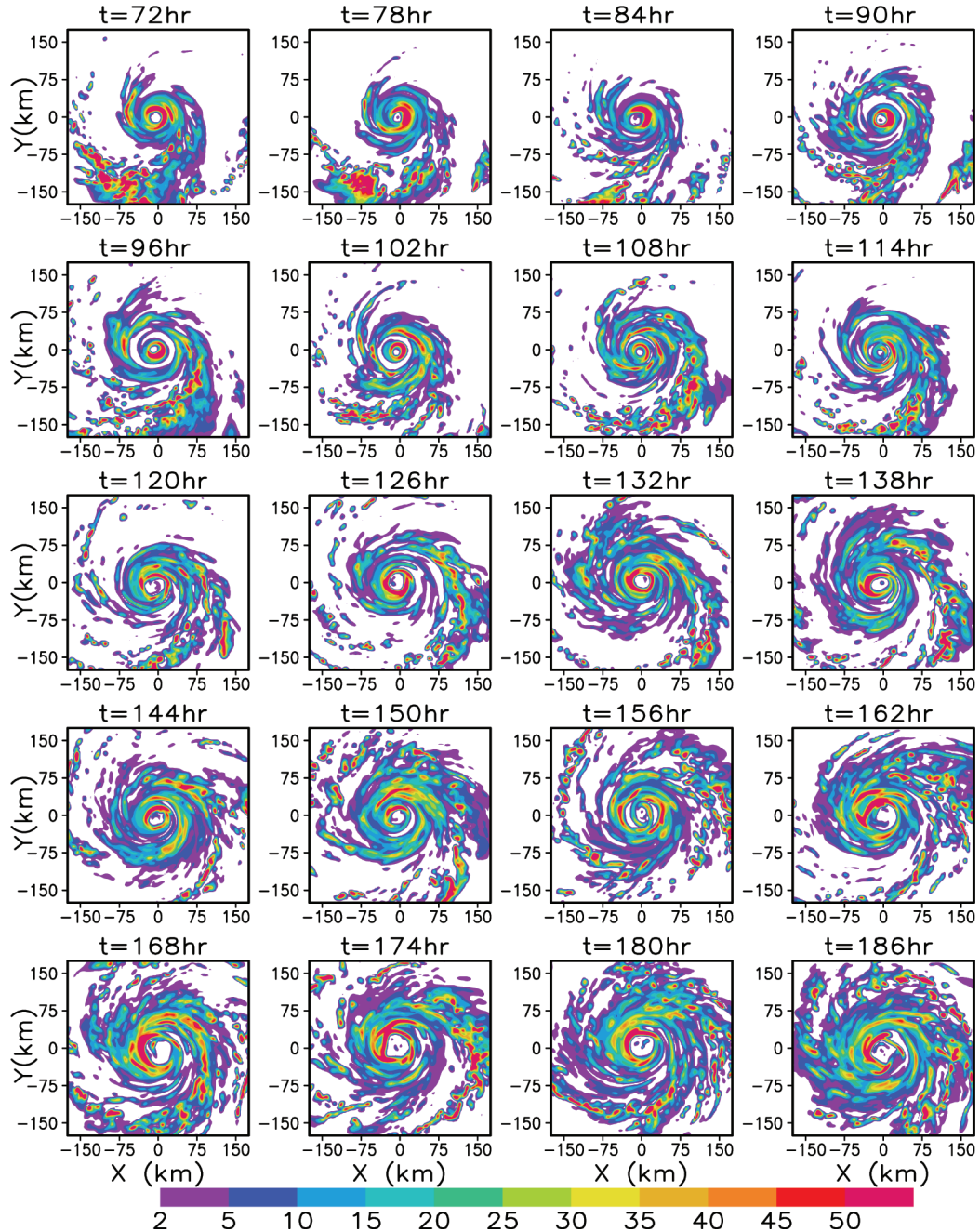


FIG. 8. 6-hourly surface rain rate (mm h^{-1}) from 72 h to 186 h of simulation for a TC on an f -plane in a 10 m/s easterly vertical shear, showing the development of active spiral rainbands and the formation of concentric eyewall and the resultant inner-core size increase of the simulated TC in TCM4 of Wang (2007).

also reported the intrusion of stratospheric air into the troposphere due to the subsidence in the eye regions (e.g., Baray et al. 1999; Carsey and Willoughby 2005; Joiner et al. 2006; de Bellevue 2007; Das 2009). It is unknown whether the high entropy air from the lower stratosphere may contribute to the warm core of an intense TC.

In addition, recent studies have demonstrated a self-stratification of the outflow layer in a TC (Emanuel and Rotunno 2011; Emanuel 2012), the studies have however focused on the radial variation outside the eyewall in the outflow layer. It is still an issue whether the mass exchange between the troposphere and the lower stratosphere may

play any roles in determining the TC structure and intensity or affecting the intensification of a TC. This issue needs to be clarified in future studies.

5. Concluding Remarks

This article has provided a literature review on recent research progress in understanding the structure and intensity of mature TCs. While the author has attempted to cover as many aspects as possible, the review could not be considered complete because some or considerable studies in this important area have not been included and also because of the rapid development of this research area in recent years. Nevertheless, this review article is expected to give an up-to-date status of the science and can be used as a reference for future studies to further advance our understanding of TC structure and intensity and their changes.

Several important aspects of TC structure have been discussed, including axisymmetric and asymmetric structures, spiral rainbands, concentric eyewall cycle, annular hurricane structure, and the inner-core size of TCs. Current understandings of the theoretical MPI and factors that limit TC maximum intensity have been summarized. Some remaining issues that need to be studied and addressed in the near future by the research community have been identified and briefly discussed. Special attention should be paid to both the inner-core dynamics and spiral rainbands in future studies. The former predominantly determines the first-order TC circulation, while the latter, including their initiation, structure, propagation, and their interaction with primary circulation and eyewall convection, play critical roles in leading to TC structure and intensity changes.

It should be pointed out that the improved understanding of many aspects of TC structure and intensity would not be possible without the rapid advancements in both in-situ and remote observations of TCs and the high-resolution numerical modeling with nonhydrostatic, cloud-revolving models. It is expected that a positive feedback among conceptual thinking, observational analysis, and more realistic modeling efforts will continue to improve our understanding of TC structure and intensity. With the improved understanding together with the advancements in observations, numerical models, data assimilation, and computing powers, forecast skills for TC structure and intensity and their changes will be continuously improved.

Acknowledgments

This study has been supported in part by US NSF grant ATM-0754039 and in part by the National Basic Research Program of China (2009CB421505) and the National Natural Science Foundation of China under Grant No. 41130964. Additional support has been provided by the JAMSTEC, NASA, and NOAA through their sponsorships of the International Pacific Research Center (IPRC) in the School of Ocean and Earth Science and Technology (SOEST) at the University of Hawaii.

References

- Abarca, S. F., and K. L. Corbosiero, 2011: Secondary eyewall formation in WRF simulation of Hurricanes Rita and Katrina (2005). *Geophys. Res. Lett.*, 38, L07802, doi:10.1029/2011GL047015.
- Baray, J. L., G. Aucellet, T. Radriambelo, and S. Baldy, 1999: Tropical cyclone Marlene and stratosphere-troposphere exchange, *J. Geophys. Res.*, 104, 13953–13970.
- Barnes, G., E. Zipser, D. Jorgensen, and F. Marks, 1983: Mesoscale and convective structure of a hurricane rainband. *J. Atmos. Sci.*, 40, 2125–2137.
- Barnes, G., J. F. Gamache, M. A. LeMone, and G. J. Stossmeister, 1991: A convective cell in a hurricane rainband. *Mon. Wea. Rev.*, 119, 776–794.
- Bell, M. M., and M. T. Montgomery, 2008: Observed structure, evolution, and potential intensity of category 5 Hurricane Isabel from 12 to 14 September. *Mon. Wea. Rev.*, 136, 2023–2046.
- Bister, M., and K. A. Emanuel, 1998: Dissipative heating and hurricane intensity. *Meteor. Atmos. Phys.*, 50, 233–240.
- Black, M. L., and H. E. Willoughby, 1992: The concentric eyewall cycle of Hurricane Gilbert. *Mon. Wea. Rev.*, 120, 947–957.
- Black, M. L., J. F. Gamache, F. D. Marks, C. E. Samsbury, H. E. Willoughby, 2002: Eastern Pacific Hurricanes Jimena of 1991 and Olivia of 1994: The Effect of Vertical Shear on Structure and Intensity. *Mon. Wea. Rev.*, 130, 2291–2312.
- Brand, S., and J. W. Bleloch, 1973: Changes in the characteristics of typhoons crossing the Philippines. *J. Appl. Meteor.*, 12, 104–109.
- Bryan, G. H., and R. Rotunno, 2009a: The influence of near-surface, high-entropy air in hurricane eyes on maximum hurricane intensity. *J. Atmos. Sci.*, 66, 148–158.
- Bryan, G. H., and R. Rotunno, 2009b: The maximum intensity of tropical cyclones in axisymmetric numerical model simulations. *Mon. Wea. Rev.*, 137, 1770–1789.
- Camp, J. P., and M. T. Montgomery, 2001: Hurricane maximum intensity: Past and present. *Mon. Wea. Rev.*, 129, 1704–1717.
- Carsey, T. P., and H. E. Willoughby, 2005: Ozone measurements from eyewall transects of two Atlantic tropical cyclones. *Mon. Wea. Rev.*, 133, 166–174.
- Chan, J. C. L., Y. Duan, and L. K. Shay, 2001: Tropical cyclone intensity change from a simple ocean-atmosphere coupled model. *J. Atmos. Sci.*, 58, 154–172.
- Chen, Y., and M. K. Yau, 2001: Spiral bands in a simulated hurricane. Part I: Vortex Rossby wave verification. *J. Atmos. Sci.*, 58, 2128–2145.
- Chou K.-H., C.-C. Wu, Y. Wang, and C.-H. Chih, 2011: Eyewall evolution of typhoons crossing the Philippines and Taiwan: An observational study. *Terr. Atmos., Oceanic Sci.*, 22, 535–548.
- Chow, K.C., K.L. Chan, and A.K.H. Lau, 2002: Generation of moving spiral bands in tropical cyclones. *J. Atmos. Sci.*, 59, 2930–2950.
- Cocks, S. B. and W. M. Gray, 2002: Variability of the outer wind profiles of western North Pacific typhoons: Classifications and techniques for analysis and forecasting. *Mon. Wea. Rev.*, 130, 1989–2005.
- Corbosiero, K. L., and J. Molinari, 2002: The effects of vertical wind shear on the distribution of convection in tropical cyclones. *Mon. Wea. Rev.*, 130, 2110–2123.
- Corbosiero, K. L., and J. Molinari, 2003: The relationship between storm motion, vertical wind shear, and convective asymmetries in tropical cyclones. *J. Atmos. Sci.*, 60, 366–460.
- Corbosiero, K. L., J. Molinari, A. R. Aiyyer, and M. L. Black, 2006: The structure and evolution of Hurricane Elena (1985). Part II: Convective asymmetries and evidence for vortex Rossby waves. *Mon. Wea. Rev.*, 134, 3073–3091.

- Cram, T. A., J. Persing, M. T. Montgomery, and S. A. Braun, 2007: A Lagrangian trajectory view on transport and mixing processes between the eye, eyewall, and environment using a high-resolution simulation of Hurricane Bonnie (1998). *J. Atmos. Sci.*, 64, 1835-1856.
- Danielsen, E. F., 1993: In situ evidence of rapid, irreversible, vertical transport of lower tropospheric air into the lower tropical stratosphere by convective cloud turrets and by larger scale upwelling in tropical cyclones, *J. Geophys. Res.-Atmosphere*, 98, 8665-8681.
- Das, S. S., 2009: A new perspective on MST radar observations of stratospheric intrusions into-troposphere associated with tropical cyclone, *Geophys. Res. Lett.*, 36, L15821, doi:10.1029/2009GL039184.
- De Bellevue, L., J., J. L. Baray, S. Baldy, G. Ancellet, R. Diab, and F. Ravetta, 2007: Simulations of stratospheric to tropospheric transport during the tropical cyclone Marlene event, *Atmos. Environ.*, 41, 6510-6526.
- DeMaria, M., and J. Kaplan, 1994: Sea surface temperature and the maximum intensity of Atlantic tropical cyclones. *J. Climate*, 7, 1324-1334.
- DeMaria, M., 1996: The effect of vertical shear on tropical cyclone intensity change. *J. Atmos. Sci.*, 53, 2076-2088.
- Diercks, J.W., and R.A. Anthes, 1976: Diagnostic studies of spiral rainbands in a nonlinear hurricane model. *J. Atmos. Sci.*, 33, 959-975.
- Dunion, J. P., and C. S. Velden. 2004: The impact of the Saharan air layer on Atlantic tropical cyclone activity. *Bull. Am. Meteor. Soc.*, 85, 353-365.
- Emanuel, K.A., 1986: An air-sea interaction theory for tropical cyclones. Part I: Steady state maintenance. *J. Atmos. Sci.*, 43, 585-604.
- Emanuel, K. A., 1988: The maximum intensity of hurricanes. *J. Atmos. Sci.*, 45, 1143-1155.
- Emanuel, K. A., 1991: The theory of hurricanes. *Annu. Rev. Fluid Mech.*, 23, 179-196.
- Emanuel, K. A., 1995: Sensitivity of tropical cyclones to surface exchange coefficients and a revised steady-state model incorporating eye dynamics. *J. Atmos. Sci.*, 52, 3969-3976.
- Emanuel, K.A., 1997: Some aspects of hurricane inner-core dynamics and energetics. *J. Atmos. Sci.*, 54, 1014-1026.
- Emanuel, K.A., 2000: A statistical analysis of hurricane intensity. *Mon. Wea. Rev.*, 128, 1139-1152.
- Emanuel, K., 2008: The Hurricane-Climate Connection. *Bull. Amer. Meteor. Soc.*, 89, ES10-ES20.
- Emanuel, K., 2012: Self-stratification of tropical cyclone outflow: Part II: Implications for storm intensification. *J. Atmos. Sci.*, 69, 988-996.
- Emanuel, K. A., C. Des Autels, C. Holloway, and R. Korty, 2004: Environmental control of tropical cyclone intensity. *J. Atmos. Sci.*, 61, 843-858.
- Emanuel, K., and R. Rotunno, 2011: Self-stratification of tropical cyclone outflow. Part I: Implications for storm structure. *J. Atmos. Sci.*, 68, 2236-2249.
- Fiorino, M., and R. L. Elsberry, 1989: Contributions to Tropical Cyclone Motion by Small, Medium and Large Scales in the Initial Vortex. *Mon. Wea. Rev.*, 117, 721-727.
- Fovell, R. G., K. L. Corbosiero, and H.-C. Kuo, 2009: Cloud microphysics impact on hurricane track as revealed in idealized experiments. *J. Atmos. Sci.*, 66, 1864-1778.
- Frank, W. M., and E. A. Ritchie, 1999: Effects of environmental flow upon tropical cyclone structure. *Mon. Wea. Rev.*, 127, 2044-2061.
- Frank, W. M., and E. A. Ritchie, 2001: Effects of vertical wind shear on the intensity and structure of numerically simulated hurricanes. *Mon. Wea. Rev.*, 129, 2249-2269.
- Frisius T., and D. Schönemann, 2012: An extended model for the potential intensity of tropical cyclones. *J. Atmos. Sci.*, 69, 641-661.
- Fudeyasu, H., and Y. Wang, 2011: Balanced contribution to the intensification of a tropical cyclone simulated in TCM4: Outer core spin-up process. *J. Atmos. Sci.*, 68, 430-449.
- Gray, W.M., 1968: Global view of the origins of tropical disturbances and storms. *Mon. Wea. Rev.*, 96, 669-700.
- Guinn, T. A., and W., H. Schubert, 1993: Hurricane spiral bands. *J. Atmos. Sci.*, 50, 3380-3403.
- Hawkins, J. D., and M. Helveston, 2008: Tropical cyclone multiple eyewall characteristics. Preprints, 28th Conf. on Hurricanes and Tropical Meteorology. Orlando, FL, Amer. Meteor. Soc., 14B.1.
- Hence, D. A., and R. A. Houze, 2008: Kinematic structure of convective-scale elements in the rainbands of Hurricanes Katrina and Rita (2005). *J. Geophys. Res.*, 113, D15108, doi:10.1029/2007JD009429.
- Hendricks, E. A., W. H. Schubert, R. K. Taft, H. Wang, and J. P. Kossin, 2009: The life cycles of hurricane-like vorticity rings. *J. Atmos. Sci.*, 66, 705-722.
- Hendricks E. A., and W. H. Schubert, 2010: Adiabatic rearrangement of hollow PV towers. *J. Adv. Model. Earth Sys.*, 2, 8, doi:10.3894/JAMES.2010.2.8
- Heymsfield, G.M., J. Halverson, E.A. Ritchie, J. Simpson, J. Molinari, and L. Tian, 2006: Structure of highly sheared Tropical Storm Chantal during CAMEX-4. *J. Atmos. Sci.*, 63, 268-287.
- Hill, K. A., and G. M. Lackmann, 2009: Influence of environmental humidity on tropical cyclone size. *Mon. Wea. Rev.*, 137, 3294-3315.
- Holland, G. J., 1997: The maximum potential intensity of tropical cyclones. *J. Atmos. Sci.*, 54, 2519-2541.
- Holland, G. J. and R. T. Merrill, 1984: On the dynamics of tropical cyclone Structural-changes. *Q. J. Roy. Meteor. Soc.*, 110, 723-745.
- Houze, R. A. Jr., S. S. Chen, B. F. Smull, W.-C. Lee, M. M. Bell, 2007: Hurricane intensity and eyewall cycle. *Science*, 315, 1235-1239.
- Huang, Y.-H., M. T. Montgomery, and C.-C. Wu, 2012: Concentric eyewall formation in Typhoon Sinlaku (2008). Part II: Axisymmetric dynamical processes. *J. Atmos. Sci.*, 69, 662-674.
- Irish, J. L., D. T. Resio, and J. J. Ratcliffe, 2008: The influence of storm size on hurricane surge. *J. Phys. Oceanogr.*, 38, 2003-2013.
- Joiner, J., A. Vasilkov, K. Yang, and P. K. Bhartia, 2006: Observations over hurricanes from the ozone monitoring instrument. *Geophys. Res. Lett.*, 33, L06807, doi:10.1029/2005GL025592.
- Judit, K., and S. S. Chen, 2010: Convectively generated potential vorticity in rainbands and formation of the secondary eyewall in Hurricane Rita of 2005. *J. Atmos. Sci.*, 67, 3581-3599.
- Kepert, J. D., 2001: The dynamics of boundary layer jets within the tropical cyclone core. Part I: Linear theory. *J. Atmos. Sci.*, 58, 2469-2484.
- Kepert, J. D., and Y. Wang, 2001: The dynamics of boundary layer jets within the tropical cyclone core. Part I: Nonlinear enhancement. *J. Atmos. Sci.*, 58, 2485-2501.
- Kimball, S. K. and M. S. Mulekar, 2004: A 15-Year Climatology of North Atlantic Tropical Cyclones. Part I: Size Parameters. *J. Climate*, 17, 3555-3575.
- Knaff, J. A., J. P. Kossin, and M. DeMaria, 2003: Annular hurricanes. *Wea. Forecasting*, 18, 204-223.
- Knaff, J. A C. R. Sampson, M. Demaria, T. P. Marchok, J. M. Gross, and C. J. McAdie, 2007: Statistical tropical cyclone wind radii prediction using climatology and persistence. *Wea. Forecasting*, 22, 781-791.

- Knaff, J. A., T. A. Cram, A. B. Schumacher, J. P. Kossin, and M. DeMaria, 2008: Objective identification of annular hurricanes. *Wea. Forecasting*, 23, 17–28.
- Kossin, J. P., and W. H. Schubert, 2001: Mesovortices, polygonal flow patterns, and rapid pressure falls in hurricane-like vortices. *J. Atmos. Sci.*, 58, 2196–2209.
- Kossin, J. P., B. D. McNoldy, and W. H. Schubert, 2002: Vortical swirls in hurricane eye clouds. *Mon. Wea. Rev.*, 130, 3144–3149.
- Kossin, J. P., and W. H. Schubert, 2004: Mesovortices in Hurricane Isabel. *Bull. Amer. Meteor. Soc.*, 85, 151–153.
- Kossin, J. P., and M. Stikowski, 2009: An objective model for identifying secondary eyewall formation in hurricanes. *Mon. Wea. Rev.*, 137, 876–892.
- Kuo, H.-C., L.-Y. Lin, C.-P. Chang, and R. T. Williams, 2004: The formation of concentric vorticity structures in typhoons. *J. Atmos. Sci.*, 61, 2722–2734.
- Kuo, H.-C., W. H. Schubert, C.-L. Tsai, and Y.-F. Kuo, 2008: Vortex interactions and barotropic aspects of concentric eyewall formation. *Mon. Wea. Rev.*, 136, 5183–5198.
- Kuo, H.-C., C.-P. Chang, Y.-T. Yang, and H.-J. Jiang, 2009: Western North Pacific typhoons with concentric eyewalls. *Mon. Wea. Rev.*, 137, 3758–3770.
- Kurihara, Y., 1976: On the development of spiral bands in a tropical cyclone. *J. Atmos. Sci.*, 33, 940–958.
- Kwon, Y. C., and W. M. Frank, 2005: Dynamic instabilities of simulated hurricane-like vortices and their impacts on the core structure of hurricanes. Part I: Dry experiments. *J. Atmos. Sci.*, 62, 3955–3973.
- Li, Q.-Q., and Y. Wang, 2012a: Formation and quasi-periodic behavior of outer spiral rainbands in a numerically simulated tropical cyclone. *J. Atmos. Sci.*, 69, 997–1020.
- Li, Q.-Q., and Y. Wang, 2012b: A comparison of inner and outer spiral rainbands in a numerically simulated tropical cyclone. *Mon. Wea. Rev.*, (in press).
- Liu, K. S., and Johnny C. L. Chan, 2002: Synoptic flow patterns associated with small and large tropical cyclones over the western North Pacific. *Mon. Wea. Rev.*, 130, 2134–2142.
- Lowag, A., M. L. Black, M. D. Eastin, 2008: Structural and intensity changes of Hurricane Bret (1999). Part I: Environmental influences. *Mon. Wea. Rev.*, 136, 4320–4333.
- Maclay, K. S., M. DeMaria, and T. H. V. Haar, 2008: Tropical cyclone inner-core kinetic energy evolution. *Mon. Wea. Rev.*, 136, 4882–4898.
- Martinez, Y., G. Brunet, and M. K. Yau, 2010: On the dynamics of two-dimensional hurricane-like concentric rings vortex formation. *J. Atmos. Sci.*, 67, 3253–3268.
- Martinez, Y., G. Brunet, M. K. Yau, and X. Wang, 2011: On the dynamics of concentric eyewall genesis: Space-time empirical normal modes diagnosis. *J. Atmos. Sci.*, 68, 457–476.
- Mei, W., C. Pasquero, and F. W. Primeau, 2012: The effect of translation speed upon the intensity of tropical cyclones over the tropical ocean. *Geophys. Res. Lett.*, doi:10.1029/2011GL050765, (in press).
- Merrill, R. T., 1984: A comparison of large and small tropical cyclones. *Mon. Wea. Rev.*, 112, 1408–1418.
- Molinari, J., and D. Vollaro, 1990: External influences on hurricane intensity. Part II: Vertical structure and response of the hurricane vortex. *J. Atmos. Sci.*, 47, 1902–1918.
- Möller, J. D., and M. T. Montgomery, 2000: Tropical cyclone evolution via potential vorticity anomalies in a three-dimensional balance model. *J. Atmos. Sci.*, 57, 3366–3387.
- Montgomery, M. T., and R. J. Kallenbach, 1997: A theory for vortex Rossby-waves and its application to spiral bands and intensity changes in hurricanes. *Q. J. Roy. Meteor. Soc.*, 123, 435–465.
- Montgomery, M. T., V. A. Vladimirov, and P.V. Denissenko, 2002: An experimental study on hurricane mesovortices. *J. Fluid Mech.*, 471, 1–32.
- Montgomery, M. T., M. M. Bell, S. D. Aberson, and M. L. Black, 2006: Hurricane Isabel (2003): New insights into the physics of intense storm. Part I: Mean vortex structure and maximum intensity estimates. *Bull. Amer. Meteor. Soc.*, 87, 1335–1347.
- Moon, Y., and D. S. Nolan, 2010: The dynamic response of the hurricane wind field to spiral rainband heating. *J. Atmos. Sci.*, 67, 1779–1805.
- Moon, Y., D. S. Nolan, and M. Iskandarani, 2010: On the use of two-dimensional flow to study secondary eyewall formation in tropical cyclones. *J. Atmos. Sci.*, 67, 3765–3773.
- Moyer, A. C., J. L. Evans, and M. Powell, 2007: Comparison of observed gale radius statistics. *Meteor. Atmos. Phys.*, 97, 41–55.
- Nolan, D. S., and M. T. Montgomery, 2002: Nonhydrostatic, three-dimensional perturbations to balanced, hurricane-like vortices. Part I: Linearized formulation, stability, and evolution. *J. Atmos. Sci.*, 59, 2989–3020.
- Nolan, D. S., Y. Moon, and D. P. Stern, 2007: Tropical cyclone intensification from asymmetric convection: Energetics and efficiency. *J. Atmos. Sci.*, 64, 3377–3405.
- Nong, S., and K. A. Emanuel, 2003: A numerical study of the genesis of concentric eyewalls in hurricanes. *Q. J. R. Meteor. Soc.*, 129, 3323–3338.
- Paterson, L.A., B.N. Hanstrum, N.E. Davidson, and H.C. Weber, 2005: Influence of environmental vertical wind shear on the intensity of hurricane-strength tropical cyclones in the Australian region. *Mon. Wea. Rev.*, 133, 3644–3660.
- Peng, M. S., B. F. Jeng, and R. T. Williams, 1999: A numerical study on tropical cyclone intensification. Part I: Beta effect and mean flow effect. *J. Atmos. Sci.*, 56, 1404–1423.
- Penn, S., 1966: Temperature and ozone variations near tropopause level over hurricane Isbell, October 1964. *J. Appl. Meteor.*, 5, 407–410.
- Persing, J., M. T. Montgomery, 2003: Hurricane superintensity. *J. Atmos. Sci.*, 60, 2349–2371.
- Powell, M. D., 1990a: Boundary layer structure and dynamics in outer hurricane rainbands. Part I: Mesoscale rainfall and kinematic structure. *Mon. Wea. Rev.*, 118, 891–917.
- Powell, M.D., 1990b: Boundary layer structure and dynamics in outer hurricane rainbands. Part II: Downdraft modification and mixed layer recovery. *Mon. Wea. Rev.*, 118, 918–938.
- Price, J. F., 1981: Upper ocean response to a hurricane. *J. Phys. Oceanogr.*, 11, 153–175.
- Qiu, X., Z.-M. Tan, and Q. Xiao, 2010: The role of vortex Rossby waves in hurricane secondary eyewall formation. *Mon. Wea. Rev.*, 138, 2092–2109.
- Reasor, P. D., M. T. Montgomery, F. D. Marks Jr., and J. F. Gamache, 2000: Low-wavenumber structure and evolution of the hurricane inner core observed by airborne dual-Doppler radar. *Mon. Wea. Rev.*, 128, 1653–1680.
- Reasor, P. D., and M. T. Montgomery, 2001: Three-dimensional alignment and corotation of weak, TC-like vortices via linear vortex Rossby waves. *J. Atmos. Sci.*, 58, 2306–2330.
- Reasor, P. D., M. T. Montgomery, and L. D. Grasso, 2004: A new look at the problem of tropical cyclones in vertical shear flow: Vortex resiliency. *J. Atmos. Sci.*, 61, 3–22.
- Riemer, M., M. T. Montgomery, and M. E. Nicholls, 2010: A new paradigm for intensity modification of tropical cyclones: Thermodynamic impact of vertical wind shear on the inflow layer. *Atmos. Chem. Phys.*, 10, 3163–3188.
- Ritchie, E. A., and W. M. Frank, 2007: Interactions between simulated tropical cyclones and an environment with variable Coriolis parameter. *Mon. Wea. Rev.*, 135, 1889–1905.

- Romps D. M., and Z. M. Kuang (2009), Overshooting convection in tropical cyclones. *Geophys. Res. Lett.*, 36, L09804, doi:10.1029/2009GL037396.
- Rotunno, R., and K. A. Emanuel, 1987: An air-sea interaction theory for tropical cyclones. Part II: Evolutionary study using a nonhydrostatic axisymmetric numerical model. *J. Atmos. Sci.*, 44, 542–561.
- Rozoff, C. M., W. H. Schubert, B. D. McNoldy, and J. P. Kossin, 2006: Rapid filamentation zones in intense tropical cyclones. *J. Atmos. Sci.*, 63, 325–340.
- Rozoff, C. M., J. P. Kossin, W. H. Schubert, and P. J. Mulero, 2009: Internal control of hurricane intensity variability: The dual nature of potential vorticity mixing. *J. Atmos. Sci.*, 66, 133–147.
- Sawada, M. and T. Iwasaki, 2010: Impacts of evaporation from raindrops on tropical cyclones. Part II: Features of rainbands and asymmetric structure. *J. Atmos. Sci.*, 67, 84–96.
- Shapiro, L. J., 1983: The asymmetric boundary layer flow under a translating hurricane. *J. Atmos. Sci.*, 40, 1984–1998.
- Schechter, D.A., and M.T. Montgomery, 2004: Damping and pumping of a vortex Rossby wave in a monotonic cyclone: Critical layer stirring versus inertia-buoyancy wave emission. *Phys. Fluids*, 16, 1334–1348.
- Schechter, D.A., and M.T. Montgomery, 2006: Conditions that inhibit the spontaneous radiation of spiral inertia-gravity waves from an intense mesoscale cyclone. *J. Atmos. Sci.*, 63, 435–456.
- Schechter, D. A., and M. T. Montgomery, 2007: Waves in a cloudy vortex. *J. Atmos. Sci.*, 64, 314–337.
- Schubert, W.H., M.T. Montgomery, R.K. Taft, T.A. Guinn, S.R. Fulton, J.P. Kossin, and J.P. Edwards, 1999: Polygonal eye-walls, asymmetric eye contraction, and potential vorticity mixing in hurricanes. *J. Atmos. Sci.*, 56, 1197–1223.
- Shade, L. R., and K. A. Emanuel, 1999: The ocean's effect on the intensity of tropical cyclones: Results from a simple coupled atmosphere-ocean model. *J. Atmos. Sci.*, 56, 642–651.
- Shea, D. J., and W. M. Gray, 1973: The hurricane's inner core region. I. Symmetric and asymmetric structure. *J. Atmos. Sci.*, 30, 1544–1564.
- Shu, S., and L. Wu. 2009: Analysis of the influence of Saharan air layer on tropical cyclone intensity using AIRS/Aqua data. *Geophys. Res. Lett.*, 36, L09809, doi:10.1029/2009GL037634.
- Smith, R. K., M. T. Montgomery, and S. Vogl, 2008: A critique of Emanuel's hurricane model and potential intensity theory. *Q. J. R. Meteor. Soc.*, 134, 551–561.
- Stern, D. P., and D. S. Nolan, 2009: Reexamining the vertical structure of tangential winds in tropical cyclones: Observations and theory. *J. Atmos. Sci.*, 66, 3579–3600.
- Stern, D. P., and D. S. Nolan, 2011: On the vertical decay rate of the maximum tangential winds in tropical cyclones. *J. Atmos. Sci.*, 68, 2073–2094.
- Stern, D. P., and D. S. Nolan, 2012: On the height of the warm core in tropical cyclones. *J. Atmos. Sci.*, 69, 1657–1680.
- Stikowski, M., J. P. Kossin, and C. M. Rozoff, 2011: Intensity and structure changes during hurricane eyewall replacement cycles. *Mon. Wea. Rev.*, 139, 3829–3847.
- Sun, D., W. K. M. Lau, M. Kafatos, Z. Boybeyi, G. Leptoukh, C. Yang, R. Yang, 2009: Numerical simulations of the impacts of the Saharan Air Layer on Atlantic tropical cyclone development. *J. Climate*, 22, 6230–6250.
- Tang, B., and K. A. Emanuel, 2010: Midlevel ventilation's constraint on tropical cyclone intensity. *J. Atmos. Sci.*, 67, 1817–1830.
- Terwey, W. D., and M. T. Montgomery, 2008: Secondary eyewall formation in two idealized, full-physics modeled hurricanes. *J. Geophys. Res.*, 113, D12112, doi:10.1029/2007JD008897.
- Wang, B., and J. C. L. Chan, 2002: How strong ENSO events affect tropical storm activity over the Western North Pacific. *J. Climate*, 15, 1643–1658.
- Wang, Y., 2001: An explicit simulation of tropical cyclones with a triply nested movable mesh primitive equation model: TCM3. Part I: Model description and control experiment. *Mon. Wea. Rev.*, 129, 1370–1394.
- Wang, Y., 2002a: Vortex Rossby waves in a numerically simulated tropical cyclone. Part I: Overall structure, potential vorticity, and kinetic energy budgets. *J. Atmos. Sci.*, 59, 1213–1238.
- Wang, Y., 2002b: Vortex Rossby waves in a numerically simulated tropical cyclone. Part II: The role in tropical cyclone structure and intensity changes. *J. Atmos. Sci.*, 59, 1239–1262.
- Wang, Y., 2007: A multiply nested, movable mesh, fully compressible, nonhydrostatic tropical cyclone model – TCM4: Model description and development of asymmetries without explicit asymmetric forcing. *Meteor. Atmos. Phys.*, 97, 93–116.
- Wang, Y., 2008a: Rapid Filamentation zone in a numerically simulated tropical cyclone. *J. Atmos. Sci.*, 65, 1158–1181.
- Wang, Y., 2008b: Structure and formation of an annular hurricane simulated in a fully compressible, nonhydrostatic model – TCM4. *J. Atmos. Sci.*, 65, 1505–1527.
- Wang, Y., 2009: How do outer spiral rainbands affect tropical cyclone structure and intensity? *J. Atmos. Sci.*, 66, 1250–1273.
- Wang, Y., and G. J. Holland, 1996: Tropical cyclone motion and evolution in vertical shear. *J. Atmos. Sci.*, 53, 3313–3332.
- Wang, Y., and C.-C. Wu, 2004: Current understanding of tropical cyclone structure and intensity changes-A review. *Meteor. Atmos. Phys.*, 87, 257–278.
- Wang, Y., and J. Xu, 2010: Energy production, frictional dissipation, and maximum intensity of a numerically simulated tropical cyclone. *J. Atmos. Sci.*, 67, 97–116.
- Weatherford, C. L., and W. M. Gray, 1988a: Typhoon structure as revealed by aircraft reconnaissance. Part I: Data analysis and climatology. *Mon. Wea. Rev.*, 116, 1032–1043.
- Weatherford, C. L., and W. M. Gray, 1988b: Typhoon structure as revealed by aircraft reconnaissance. Part II: Structural variability. *Mon. Wea. Rev.*, 116, 1044–1056.
- Willoughby, H. E., 1978: A Possible Mechanism for the formation of hurricane rainbands. *J. Atmos. Sci.*, 35, 838–848.
- Willoughby, H. E., J. A. Clos, and M. G. Shoreibah, 1982: Concentric eyewalls, secondary wind maximum, and the evolution of the hurricane vortex. *J. Atmos. Sci.*, 39, 395–411.
- Willoughby, H. E., F. D. Marks Jr., and R. J. Feinberg, 1984a: Stationary and moving convective bands in hurricanes. *J. Atmos. Sci.*, 41, 505–514.
- Willoughby, H. E., H.-L. Jin, S. J. Lord, and J. M. Piotrowicz, 2004b: Hurricane structure and evolution as simulated by an axisymmetric, nonhydrostatic numerical model. *J. Atmos. Sci.*, 61, 1169–1186.
- Wong, M. L. M., and J. C. L. Chan, 2004: Tropical cyclone intensity in vertical wind shear. *J. Atmos. Sci.*, 61, 1859–1876.
- Wu, C.-C., K.-H. Chou, H.-J. Cheng, and Y. Wang, 2003: Eyewall contraction, breakdown and reformation in a landfalling typhoon. *Geophys. Res. Lett.*, 30, L1887, doi:10.1029/2003GL017653.
- Wu, C.-C., C.-Y. Lee, I.-I. Lin, 2007: The effect of the ocean eddy on tropical cyclone intensity. *J. Atmos. Sci.*, 64, 3562–3578.
- Wu, L., 2007: Impact of Saharan air layer on hurricane peak intensity. *Geophys. Res. Lett.*, 34, L09802, doi:10.1029/2007GL029564.
- Wu, L., and S. A. Braun, 2004: Effects of environmentally induced asymmetries on hurricane intensity: A numerical study. *J. Atmos. Sci.*, 61, 3065–3081.
- Wu, L., S. A. Braun, J. J. Qu, and X. Hao, 2006: Simulating the formation of Hurricane Isabel (2003) with AIRS data. *Geo-*

- phys. Res. Lett.*, 33, L04804, doi:10.1029/2005GL024665.
- Xu, J., and Y. Wang, 2010a: Sensitivity of tropical cyclone inner core size and intensity to the radial distribution of surface entropy flux. *J. Atmos. Sci.*, 67, 1831-1852.
- Xu, J., and Y. Wang, 2010b: Sensitivity of the simulated tropical cyclone inner-core size to the initial vortex size. *Mon. Wea. Rev.*, 138, 4135-4157.
- Yang, B., Y. Wang, and B. Wang, 2007: The effect of internally generated inner core asymmetric structure on tropical cyclone intensity. *J. Atmos. Sci.*, 64, 1165-1188.
- Yu, C.-K., and C.-L. Tsai, 2010: Surface pressure features of land-falling typhoon rainbands and their possible causes. *J. Atmos. Sci.*, 67, 2893-2911.
- Zeng, Z., Y. Wang, and C.-C. Wu, 2007: Environmental dynamical control of tropical cyclone intensity-An observational study. *Mon. Wea. Rev.*, 135, 38-59.
- Zeng, Z., L.-S. Chen, and Y. Wang, 2008: An observational study of environmental dynamical control of tropical cyclone intensity in the North Atlantic. *Mon. Wea. Rev.*, 136, 3307-3322.
- Zeng, Z.-H., Y. Wang, and L.-S. Chen, 2010: A statistical analysis of vertical shear effect on tropical cyclone intensity change in the North Atlantic. *Geophys. Res. Lett.*, 37, L02802, doi:10.1029/2009GL041788.
- Zhan, R.-F., Y. Wang, and X.-T. Lei, 2011: Contributions of ENSO and East Indian Ocean SSTA to the interannual variability of Northwest Pacific tropical cyclone frequency. *J. Climate*, 24, 509-521.
- Zhang, D.-L., and C.Q. Kieu, 2006: Potential vorticity diagnosis of a simulated hurricane. Part II: Quasi-balanced contributions to forced secondary circulations. *J. Atmos. Sci.*, 63, 2898-2914.
- Zhou, X., and B. Wang, 2009: From concentric eyewall to annular hurricane: A numerical study with the cloud-resolved WRF model. *Geophys. Res. Lett.*, 36, DOI:10.1029/2008GL036854.
- Zhou, X., and B. Wang, 2011a: Impact of secondary eyewall heating on tropical cyclone intensity change. *J. Atmos. Sci.*, 68, 450-456.
- Zhou, X., and B. Wang, 2011b: Mechanism of concentric eyewall replacement cycles and associated intensity change. *J. Atmos. Sci.*, 68, 972-988.
- Zhu, H., W. Ulrich, and R. K. Smith, 2004: Ocean effects on tropical cyclone intensification and inner-core asymmetries. *J. Atmos. Sci.*, 61, 1245-1258.
- Zhu, T., D.-L. Zhang, and F. Weng, 2004: Numerical simulation of Hurricane Bonnie (1998). Part II: Eyewall evolution and intensity changes. *Mon. Wea. Rev.*, 132, 225-241.